

Supporting Information

Rhodamine-Derived Ratiometric Fluorescent Probes for High-Sensitivity Detection and Real-Time Imaging of Mitochondrial pH and Viscosity in HeLa Cells and *Drosophila Melanogaster*

Subash Pandey, Dilka Liyana Arachchige, Ronald J. Schwandt, Sushil K. Dwivedi, Ishana Kathuria, Haiying Liu, and Rudy L. Luck*

Department of Chemistry, Michigan Technological University, Houghton, MI 49931.

*Corresponding author.

*E-mail: rluck@mtu.edu

Table of Contents

1. Reagents:	5
2. Instrumentation	5
3. Synthesis	5
Synthesis of compound 1	5
Synthesis of compound 2	6
Synthesis of compound 3	6
Synthesis of probe A	6
Synthesis of probe B	6
4. Selectivity and Photostability Study	7
5. Cytotoxicity of probe A	7
6. $^1\text{H-NMR}$, $^{13}\text{C-NMR}$ spectra, and LC-MS of compounds.	8
Figure S1. ^1H NMR spectrum of compound 1 in CDCl_3	8
Figure S2. ^1H NMR spectrum of compound 2 in CDCl_3	8
Figure S3. ^1H NMR spectrum of compound 3 in CDCl_3	9
Figure S4. ^{13}C NMR spectrum of compound 3 in CDCl_3	9
Figure S5. ^1H NMR spectrum of probe A in CDCl_3	10
Figure S5a. ^1H NMR of probe A in closed ring form in DMSO-d_6	10
Figure S5b. ^1H NMR of probe A in open ring form in DMSO-d_6 and 1 equivalent of trifluoroacetic acid (TFA).....	11
Figure S5c. ^1H NMR of probe A in open ring form in DMSO-d_6 with 2 equivalents of trifluoroacetic acid (TFA).....	11
Figure S6. ^{13}C NMR spectrum of probe A in CDCl_3	12
Figure S7. Electrospray ionization (ESI) MS spectrum (top) with expanded region (bottom) probe A	13
Figure S8. MALDI TOF MS spectrum of probe A	14
Figure S9. ^1H NMR spectrum of probe B in CDCl_3	14
Figure S10. ^{13}C NMR spectrum of probe B in CDCl_3	15
Figure S11. Electrospray ionization (ESI) MS spectrum of probe B	15
Figure S12. MALDI TOF MS spectrum of probe B	16
7. FTIR of probes A and B	16
Figure S13. FTIR spectra of probes A and B	16
8. Tauc plot for probe A	17
Figure S14. Tauc Plot for probe A under acidic (left) and basic pH (right) conditions.	17
9. UV-Vis and Fluorescence spectra of probe B	17

Figure S15. (a) Absorption and (b) fluorescence spectra with excitation at 325 nm of probe B (10 mM) recorded in various pH buffer solutions containing 30% DMSO.....	17
Figure S16. pKa calculation of (a) Probe A , and (b) Probe B using sigmoidal Boltzmann fitting method.....	18
11. Selectivity test and Photostability test for probes A and B	18
Figure S17. Fluorescence intensity of Probe A in the absence and presence of 50 μ M of various (a) metal ions, (b) anions and (c) amino acids. Measurements were taken at pH levels of 7.2 using PBS buffer under excitation at 400 nm. Rhodamine emission peak at 660 nm is used to compare the emission intensity of probe A . (d) Photostability of probe A in acidic, neutral and basic pH for 125 minutes.....	19
Figure S18. Fluorescence intensity of probe B in the absence and presence of 50 μ M of various (a) metal ions, (b) anions and (c) amino acids. Measurements were taken at pH levels of 7.2 using PBS buffer under excitation at 380 nm. The emission peak at 570 nm is used to compare the emission intensity of probe B in different cations, anions, and amino acids. (d) Photostability of probe B in acidic, neutral and basic pH for 125 minutes.....	20
12. Reversibility test for probe A	20
Figure S19. Reversibility test of Probe A between pH 3.3 and 6.93 for 10 cycles.....	21
13. Theoretical Calculations	21
Figure S20. The structure of probe A as displayed in a Mercury ⁵ drawing.....	21
Figure S21. Overlay of the calculated structures for probes A (blue) and AH ⁺ (red).	22
Table S1. Calculated atomic coordinates for probe A	22
Figure S22. Calculated vibrational spectrum for probe A	24
Figure S23. Calculated UV-Vis spectrum for probe A	24
Table S2. Excitation energies and oscillator strengths listing for probe A	24
Figure S24. LCAOs for probe A involved with the transition noted as Excited States 1, 4, and 6 in Table S2.	26
Figure S25. Mercury ⁵ representation of probe AH ⁺	26
Table S3. Calculated atomic coordinates for probe AH ⁺	26
Figure S26. Calculated vibrational spectrum for probe AH ⁺	27
Figure S27. Calculated UV-Vis spectrum for probe AH ⁺	28
Table S4. Excitation energies and oscillator strengths listing for probe AH ⁺	28
Figure S28. LCAOs for probe AH ⁺ involved with the transition noted as Excited States 1, 2 and 6 in Table S4.	29
Figure S29. The structure of probe B as displayed in a Mercury ⁵ drawing.....	30
Figure S30. Overlay of the calculated structures for probes B (blue) and BH ⁺ (red).....	30
Table S5. Calculated atomic coordinates for probe B	31
Figure S31. Calculated vibrational spectrum for probe B	32
Figure S32. Calculated UV-Vis spectrum for probe B	33

Table S6. Excitation energies and oscillator strengths listing for probe B	33
Figure S33. LCAOs for probe B involved with the transition noted as Excited States 1 and 7 in Table S10.	34
Figure S34. Mercury ⁵ representation of probe BH ⁺	35
Table S7. Calculated atomic coordinates for probe BH ⁺	35
Figure S35. Calculated vibrational spectrum for probe BH ⁺	37
Figure S36. Calculated UV-Vis spectrum for probe BH ⁺	37
Table S8. Excitation energies and oscillator strengths listing for probe BH ⁺	37
Figure S37. LCAOs for probe BH ⁺ involved with the transition noted as Excited State 1 in Table S12.	38
Figure S38. Current density difference drawings as isosurfaces of probes B (left) and BH ⁺ (right). The number of excited states (ES), the calculated (and experimental) wavelengths, and the transitions together with percentage contributions are listed. The range values for the color scale illustrated at the top of the figure are also listed.....	40
14. Colocalization study in HeLa cells using Lysosome Tracker	41
Figure S39. Fluorescence images of HeLa cells incubated for 2 hours with 10 μ M probe A . The green channel (I) was used to observe the visible fluorescence of probes A in the 425-525 nm range, while the red channel (II) captured the near-infrared fluorescence from probe A (600-700 nm). Green channels utilized Alexa Fluor 405 nm and red channels utilized Alexa Fluor 559 nm excitation. The magenta channel (III) is used to detect near-infrared fluorescence from the lysosome-specific dye in the 700-800 nm range with Alexa Fluor 635 nm excitation. Scale bars represent 20 μ m.....	41
Figure S40. HeLa cells were first incubated with probe A and Lysotracker in DMEM for 30 minutes, followed by imaging using a confocal fluorescence microscope. Subsequently, the cells were treated with 5 μ M rapamycin for 30, 45, 90, 105, and 120 minutes, and fluorescence images were acquired at each time period.....	42
Figure S41. Measurement of the zeta potential of probe A in DMSO.....	43
Table S9. Comparison of the proposed probe with other reported mitochondria targeting pH probes.....	44
Figure S42: Fluorescence intensity of Probe A (left) and Probe B (right) in the absence and presence of 100 μ M of peroxynitrite, H ₂ O ₂ , and 100 μ L of H ₂ S gas in PBS solution. Measurements were taken at pH levels of 7.2 using PBS buffer under excitation at 380 nm, and 400 nm, respectively. The rhodamine emission peak at 660 nm is used to indicate the emission intensity of probe A and the emission peak at 570 nm is used for the emission intensity of probe B	46
Figure S43. UV-visible spectra of synthesized peroxynitrite.	47
Figure S44. Fluorescence spectra of probe AH ⁺ in buffer (pH 3.50) with varying glycerol concentrations.	48
15. References	49

1. Reagents:

6-amino-3,4-dihydronaphthalen-1(2H)-one, methyl iodide (CH_3I), 2-(3-(diethylamino)-2-hydroxybenzoyl)benzoic acid, hydrazine ($\text{NH}_2\text{-NH}_2$), benzotriazole-1-yl-oxy-tris-(dimethylamino)-phosphonium hexafluorophosphate (BOP), 4-Chloro-7-nitrobenzofurazan, and 7-(diethylamino)-2-oxo-3,8a-dihydro-2H-chromene-3-carbaldehyde were procured from MilliporeSigma. All other reagents were purchased from different commercial vendors with analytical grades and utilized in their original form. The aqueous solutions were prepared using nanopure water ($18.2 \text{ M}\Omega \text{ cm}$, Millipore Inc.).

2. Instrumentation

^{13}C (125 MHz) and ^1H NMR (500 MHz) spectra were recorded using a Bruker NMR spectrometer (Ascend 500) in CDCl_3 . pH values of buffers were measured with a Fisherbrand Accumet Basic AB315 Benchtop Laboratory pH/mV Meter at 25 °C. Absorption and fluorescence spectra were obtained on a PerkinElmer Lambda 35 UV/vis spectrometer (850 nm to 300 nm, medium scan speed, and a 0.5 nm sampling interval) and Jobin Yvon Fluoromax-4 spectrofluorometer (5 nm entrance slit and exit slit, and 1200.00 g/mm grating), respectively. The fluorescence images of probe A were collected using an Olympus FluoView FV1000 confocal fluorescence microscope (Olympus America Inc., 60x objective lens). Cellular images were analyzed and processed with an Olympus FV10-ASW 3.1 viewer, ImageJ Fiji, and Photoshop 6.0.

3. Synthesis

Synthesis of compound 1.

The synthesis of compound **1** was reported previously and we modified this procedure.¹ 6-amino-3,4-dihydronaphthalen-1(2H)-one (2 g, 12.4 mmol) was added to a solution of 40 mL degassed dimethyl formamide (DMF), 8.3 g of methyl iodide, (CH_3I , 58.47 mmol) and 3.18 g of potassium carbonate (K_2CO_3 , 23.0 mmol), see Scheme 1. The mixture was heated at 45°C for 12 hours under an N_2 atmosphere. After cooling to room temperature, the mixture was concentrated, and water and ethyl acetate (EtOAc) were added for the extraction of the compound. The aqueous layer with water-soluble impurities was discarded, and the organic layer was washed several times with water. The rinsed upper organic layer was separated, dried with Na_2SO_4 , filtered, and the solvent removed using a rotary evaporator. The crude product was purified by column chromatography with a hexane and EtOAc mixture in a 7:1 ratio. The compound appeared pale yellow on the column and colorless in solution. The colorless solution is then dried completely yielding a white product (1.740 g, yield: 74%). ^1H NMR (500 MHz, CDCl_3) δ (ppm): 7.97 (d, $J = 10.0 \text{ Hz}$, 1H), 6.61 (d, $J = 15.0 \text{ Hz}$, 1H), 6.41 (s, 1H), δ 3.07 (s, 6H), 2.90 (t, $J = 5.0 \text{ Hz}$, 2H), 2.59 (t, $J = 10.0 \text{ Hz}$, 2H), δ 2.11 (m, 2H).

Synthesis of compound 2

Compound **1** (1 g, 5.28 mmol), and 2-(3-(diethylamino)-2-hydroxybenzoyl)benzoic acid (1.5 g, 4.8 mmol) were refluxed in 20 mL of concentrated H_2SO_4 for 12 hours under a nitrogen atmosphere, see Scheme 1. The reaction was cooled to room temperature and some ice cubes were added. 5 mL of perchloric acid (HClO_4) was then added dropwise until a precipitate appeared. More ice cubes were added and the precipitate obtained by vacuum filtration. The precipitate was washed with small amounts of nanopurified water, dried and collected resulting in a red color product (2.10 g, yield: 85%). ^1H NMR (500 MHz, CDCl_3) δ (ppm): ^1H NMR (500 MHz, CDCl_3)

δ (ppm): 8.30 (d, $J = 11.3$ Hz, 1H), 8.19 (d, $J = 10.0$ Hz, 1H), 7.77 (t, $J = 3.6$ Hz, 1H), 7.67 (t, $J = 7.6$ Hz, 1H), 7.24 (d, $J = 7.4$ Hz, 1H), 6.93 (m, 2H), 6.82 (t, $J = 10.0$ Hz, 2H), 6.54 (s, 1H), 3.57 (q, $J = 10.0$ Hz, 4H), 3.40 (m, 1H), 3.21 (s, 6H), 2.90 (m, 3H), 1.32 (t, $J = 10.0$ Hz, 6H).

Synthesis of compound 3

1.66 g (3.547 mmol) of compound **2** was dissolved in 20 mL of degassed DCM containing 1.568 g (3.547 mmol) of BOP and stirred at room temperature for 1 hour under an N₂ atmosphere. 568 μ L (17.725 mmol) of hydrazine was added using a syringe and the resultant mixture stirred for 2 hours. The crude product was extracted using dichloromethane, dried using Na₂SO₄, and concentrated. The final product was purified using column chromatography (silica gel, particle size 0.063–0.2 mm, Merck) and eluted using a hexane and ethyl acetate mixture in a 3:7 ratio. The resulting product is light green (900 mg, yield: 53 %). ¹H NMR (500 MHz, CDCl₃), δ (ppm): 7.94 (d, $J = 6.6$ Hz, 1H), 7.75 (d, $J = 8.6$ Hz, 1H), 7.51 (m, 2H), 7.24 (d, $J = 6.7$ Hz, 1H), 6.67 (d, $J = 8.6$ Hz, 1H), 6.52 (s, 1H), 6.48 (s, 1H), 6.40 (d, $J = 8.8$ Hz, 1H), 6.32 (d, $J = 8.9$ Hz, 1H), 3.69 (s, 2H), 3.37 (q, $J = 7.1$ Hz, 4H), 3.01 (s, 6H), 2.70 (m, 2H), 1.86 (m, 1H), 1.69 (m, 1H), 1.28 (t, $J = 7.2$ Hz, 1H), 1.20 (t, $J = 7.1$ Hz, 6H). ¹³C NMR (125 MHz, CDCl₃), δ (ppm): 166.40, 153.57, 150.79, 149.65, 148.80, 147.87, 138.04, 132.43, 130.87, 123.27, 118.47, 111.40, 109.89, 108.59, 104.07, 100.06, 99.50, 98.18, 67.57, 63.72, 60.47, 44.42, 40.52, 28.98, 21.30, 14.28, 12.71.

Synthesis of probe A

Compound **3** (320 mg, 0.665 mmol) was added to 20 mL of degassed methanol containing 4-Chloro-7-nitrobenzofurazan (132.7 mg, 0.665 mmol). The solution was stirred for 24 hours at room temperature under an N₂ environment, Scheme 1. The reaction solvent was removed in vacuo. The crude product was purified by column chromatography (silica gel, particle size 0.063–0.2 mm, Merck). It was eluted using a hexane and ethyl acetate gradient mixture in ratios from 9:1 to 1:1. This process resulted in pure probe **A** which was green in color (265 mg, yield: 62%, m.p.: 195 °C). ¹H NMR (500 MHz, CDCl₃), δ (ppm): 8.30 (d, $J = 7.6$ Hz, 1H), 8.05 (d, $J = 6.6$ Hz, 1H), 7.68 (t, $J = 8.0$ Hz, 1H), 7.61 (t, $J = 7.1$ Hz, 1H), 7.34 (d, $J = 7.6$ Hz, 1H), 6.59 (d, $J = 8.8$ Hz, 1H), 6.47 (m, 2H), 6.36 (m, 3H), 3.37 (q, $J = 6.4$ Hz, 4H), 3.00 (s, 6H), 2.70 (t, $J = 7.0$ Hz, 2H), 1.99 (s, 2H), 1.19 (t, $J = 7.0$ Hz, 6H). ¹³C NMR (125 MHz, CDCl₃), δ (ppm): 166.39, 153.51, 150.73, 149.58, 148.75, 147.84, 137.97, 133.40, 132.40, 130.75, 128.35, 127.91, 125.28, 124.62, 123.57, 123.21, 122.99, 118.38, 116.60, 110.70, 111.28, 110.63, 109.78, 108.53, 103.93, 99.37, 98.12, 67.58, 60.41, 44.41, 44.35, 40.44, 40.30, 40.14, 28.91, 21.21, 12.71, 12.64, 12.53. *m/z* = 643.25.

Synthesis of probe B

Compound **3** (200 mg, 0.540 mmol) was added to 20 mL of degassed ethanol containing 7-(diethylamino)-2-oxo-3,8a-dihydro-2H-chromene-3-carbaldehyde (133.5 mg, 0.540 mmol). The solution was stirred for 24 hours at room temperature under N₂ environment, Scheme 1. The reaction solvent was removed in vacuo. The crude product was purified by column chromatography (silica gel, particle size 0.063–0.2 mm, Merck). It was eluted using a hexane and ethyl acetate gradient mixture in ratios from 9:1 to 1:1. This process resulted in pure probe **B** as a dark mustard yellow product (191 mg, yield: 50%, m.p.: 186 °C). ¹H NMR (500 MHz, CDCl₃), δ (ppm): 8.71 (s, 1H), 8.22 (s, 1H), 8.00 (d, $J = 7.4$ Hz, 1H), 7.83 (d, $J = 8.6$ Hz, 1H), 7.53 (m, 2H), 7.23 (m, 2H), 6.67 (d, $J = 7.5$ Hz, 1H), 6.51 (m, 4H), 6.37 (d, $J = 2.4$ Hz, 1H), 6.28 (d, $J = 8.9$ Hz, 1H), 3.36 (m, 8H), 2.98 (s, 6H), 2.65 (m, 2H), 1.95 (m, 1H), 1.68 (m, 1H), 1.18 (m, 12H). ¹³C NMR (125 MHz, CDCl₃), δ (ppm): 165.23, 161.42, 156.93, 152.58, 151.14, 150.75, 150.61,

148.89, 146.96, 142.04, 138.42, 138.06, 133.32, 130.30, 129.55, 128.51, 127.87, 123.56, 123.52, 123.34, 118.54, 114.83, 111.35, 109.98, 109.19, 108.81, 108.56, 105.31, 100.82, 100.06, 98.40, 97.10, 67.72, 60.47, 44.92, 44.36, 40.53, 40.27, 28.86, 21.28, 21.13, 14.29, 12.75, 12.66, 12.57. m/z = 709.36.

4. Selectivity and Photostability Study

The selectivity tests were performed using 50 μ M biologically related cationic analytes (Al^{3+} , Fe^{3+} , Sn^{2+} , Na^+ , K^+ , Zn^{2+} , Co^{2+} , Cu^{2+} , Mg^{2+}), anionic analytes (PO_4^{3-} , acetate, Cl^- , SO_4^{2-} , NO_2^- , I^- , SO_3^{2-} , CN^- , NO_3^- , CO_3^{2-}), and various amino acids (glycine, tyrosine, serine, lysine, arginine, cystine, cysteine, glutathione, alanine, valine, and methionine) in PBS buffer. The photochemical stability was examined at three different pH values: 4.40, 6.90, and 8.80.

5. Cytotoxicity of probe A

HeLa cells were cultured in Thermo Scientific™ BioLite™ Cell Culture treated dishes at 37°C in a humidified incubator with a 5% CO_2 atmosphere and allowed to grow until 80% confluence was attained. The cells were cultured in Dulbecco's modified Eagle's medium (DMEM) supplemented with 10% fetal bovine serum (FBS), penicillin, and streptomycin in 5:1:1 ratio. HeLa cells were seeded in a 96-well plate at a density of 1×10^5 cells per well and allowed to adhere for 24 hours. Subsequently, cells were treated with various concentrations of probe A (0, 10, 20, 30, 40, and 50 μ M) for 12 hours. After exposure, 100 μ L of MTT solution (5 mg/mL in PBS) was added to each well and the cells were incubated for 4 hours. The resulting formazan crystals were solubilized with 100 μ L of DMSO, and the absorbance was measured at 570 nm using a microplate reader. Cell viability was assessed using the formula,

$$V_{\text{rate}} = \frac{(A - AB)}{(AC - AB)} \times 100\%$$

where A represents the absorbance of the cells treated with various concentrations of probe A, AC is the absorbance of the control cell medium, and AB is the blank group without cells.

6. $^1\text{H-NMR}$, $^{13}\text{C-NMR}$ spectra, and LC-MS of compounds.

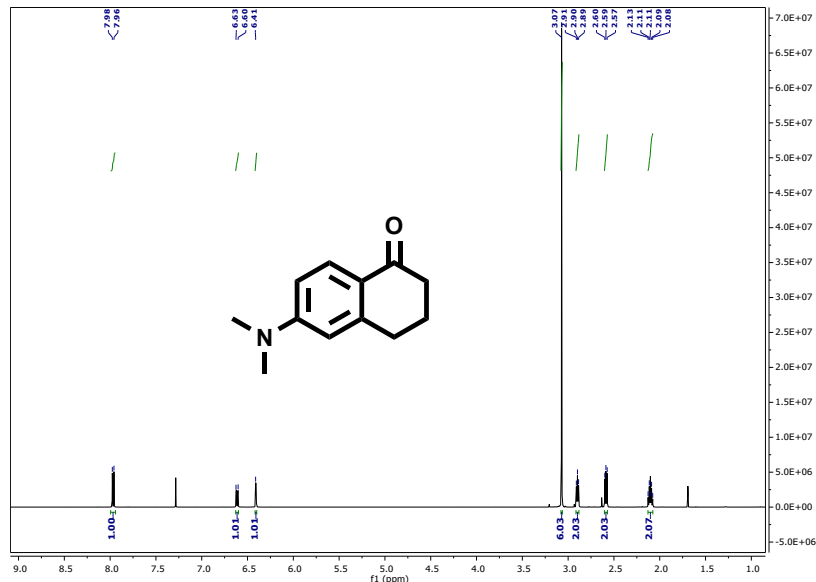


Figure S1. ^1H NMR spectrum of compound **1** in CDCl_3 .

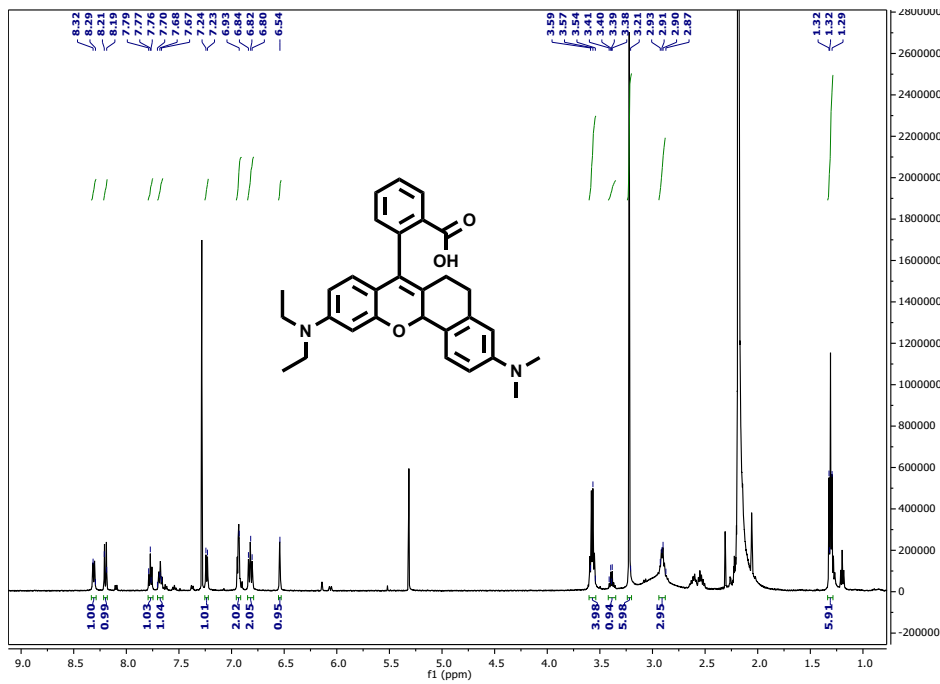


Figure S2. ^1H NMR spectrum of compound **2** in CDCl_3 .

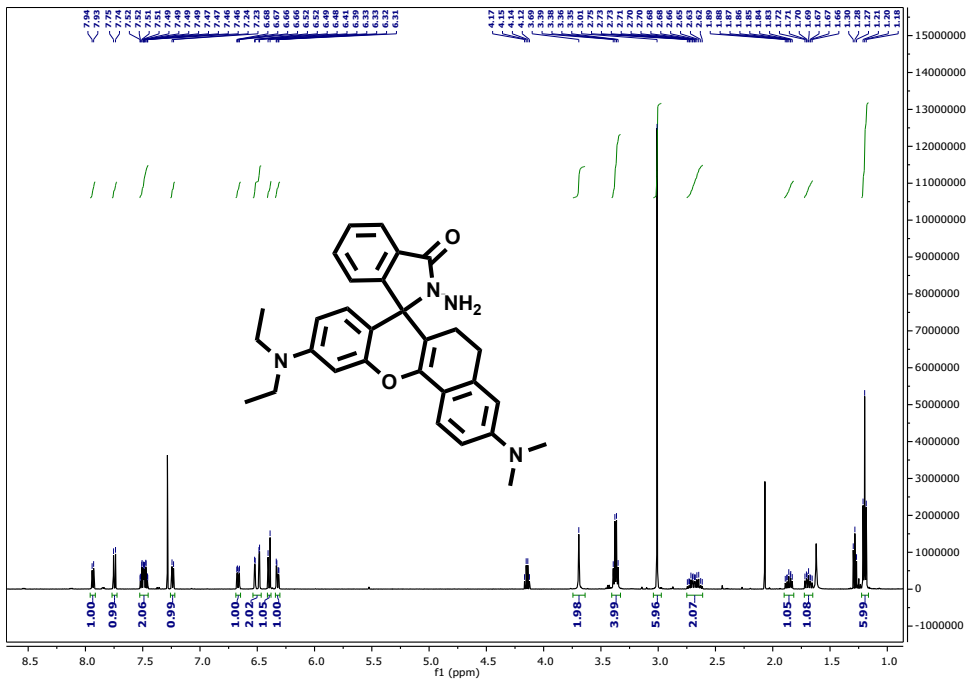


Figure S3. ^1H NMR spectrum of compound **3** in CDCl_3 .

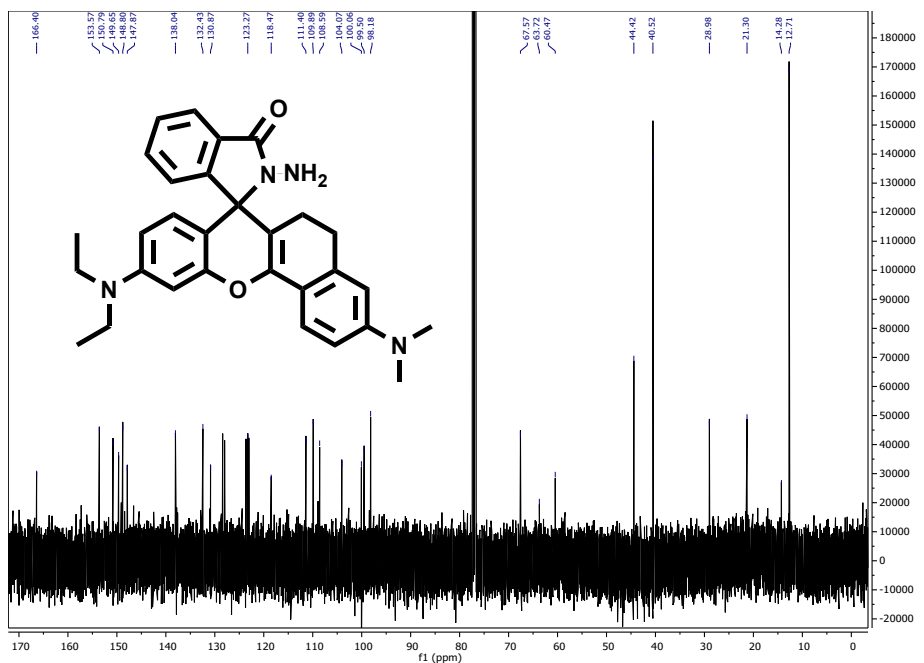


Figure S4. ^{13}C NMR spectrum of compound **3** in CDCl_3 .

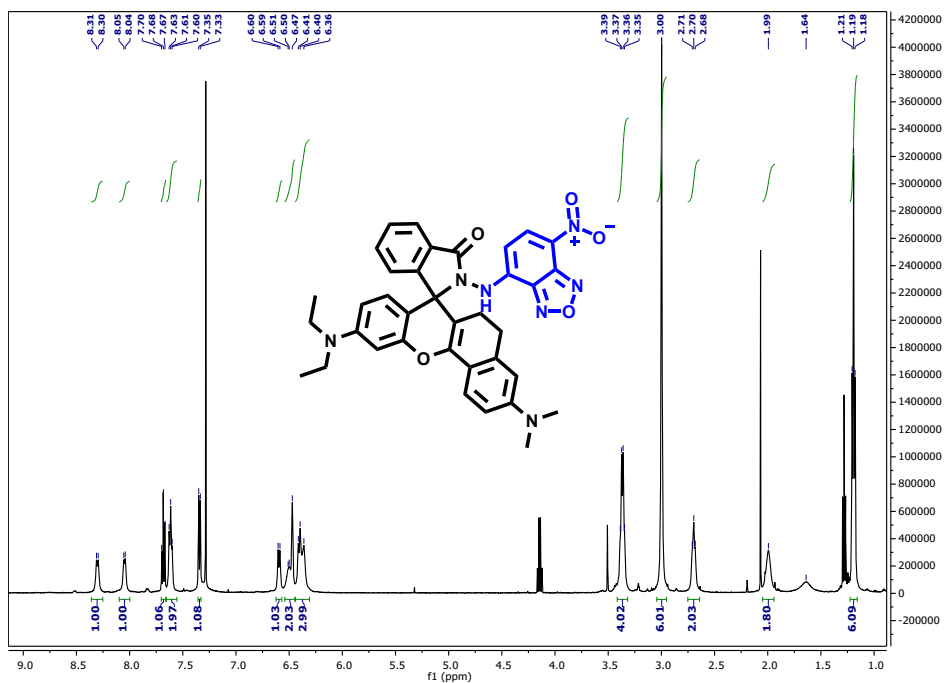


Figure S5. ^1H NMR spectrum of probe A in CDCl_3 .

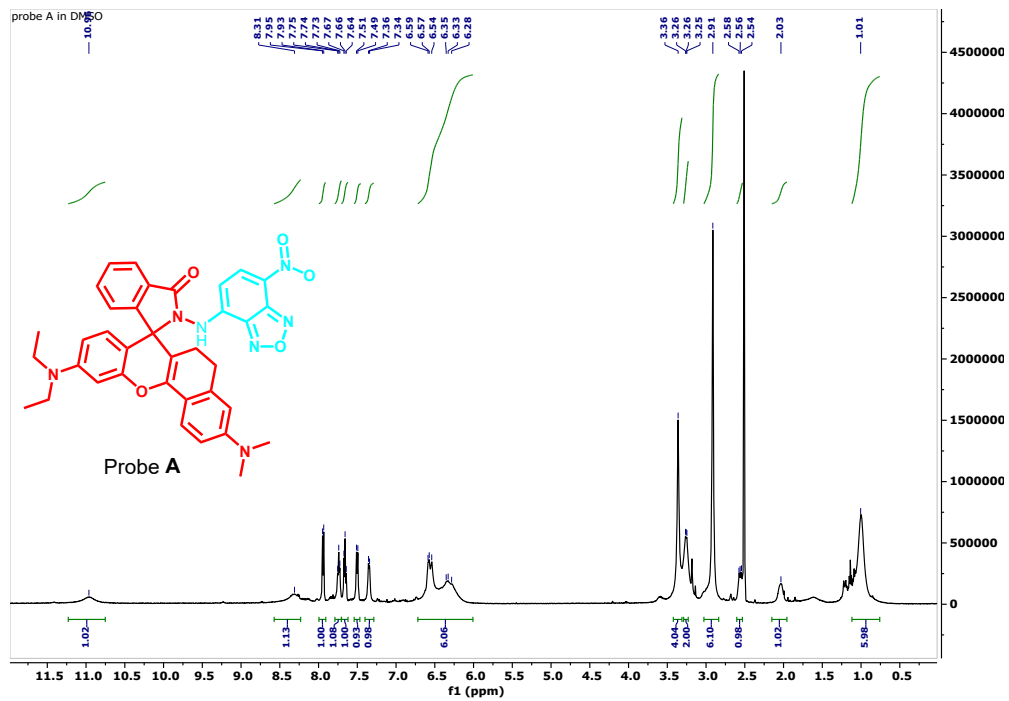


Figure S5a. ¹H NMR of probe A in closed ring form in DMSO-d₆.

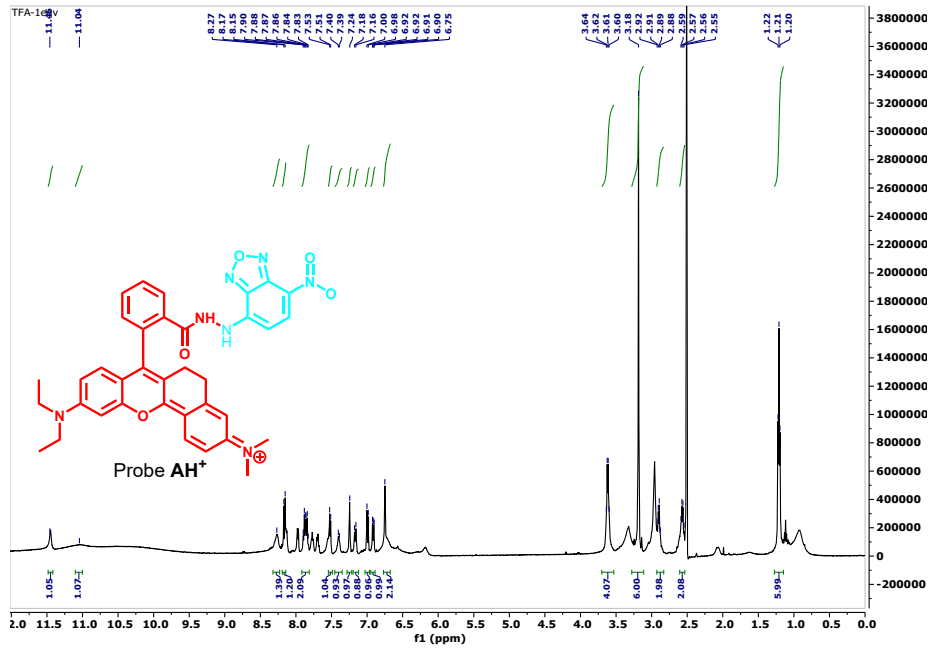


Figure S5b. ¹H NMR of probe A in open ring form in DMSO-d₆ and 1 equivalent of trifluoroacetic acid (TFA).

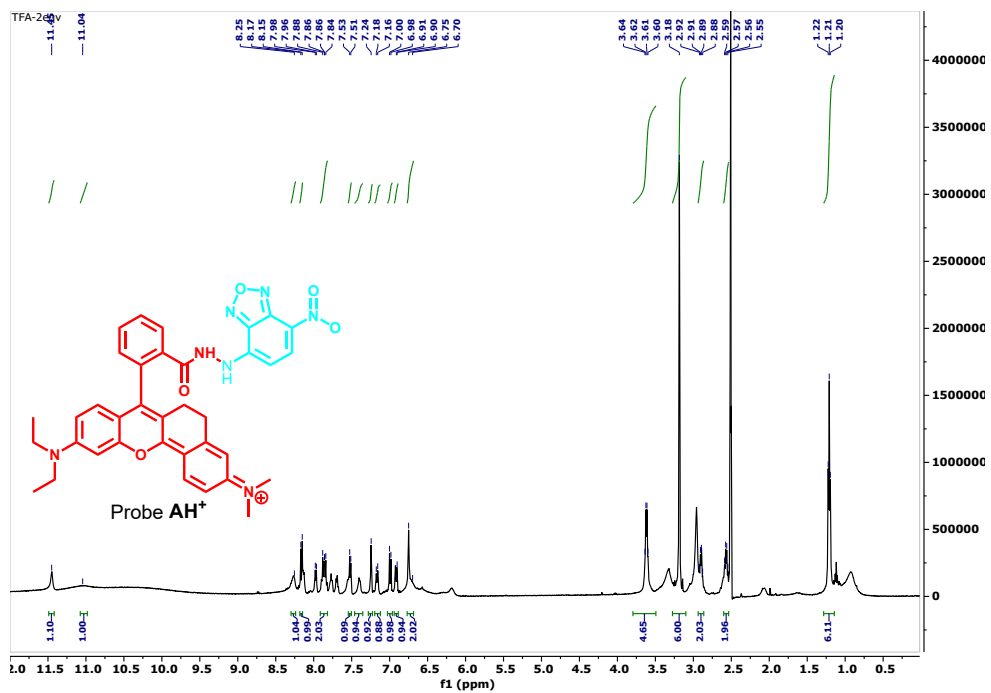


Figure S5c. ¹H NMR of probe A in open ring form in DMSO-d6 with 2 equivalents of trifluoroacetic acid (TFA).

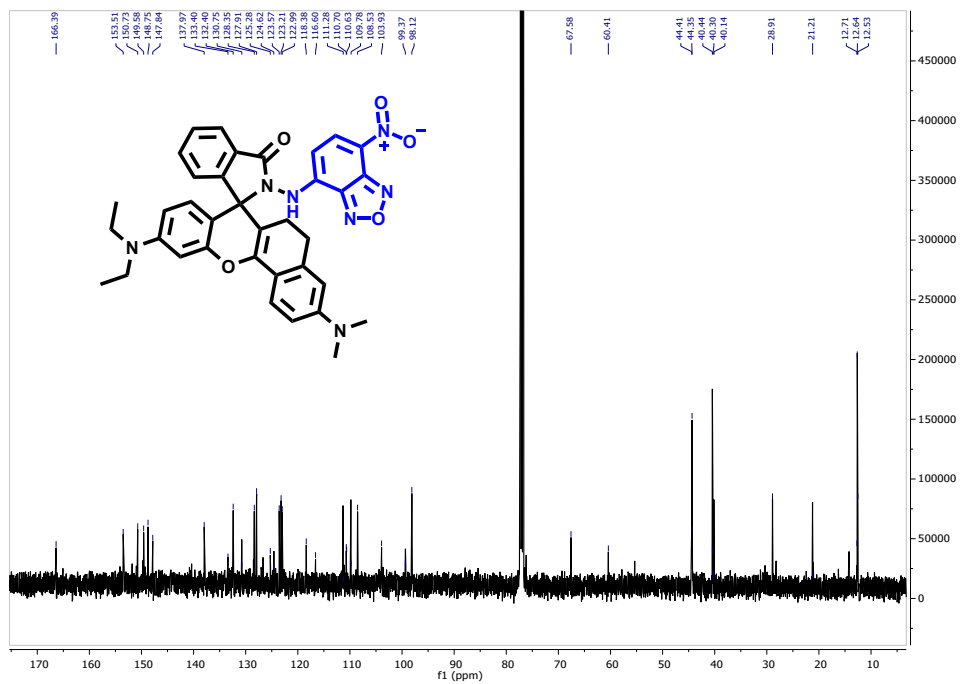
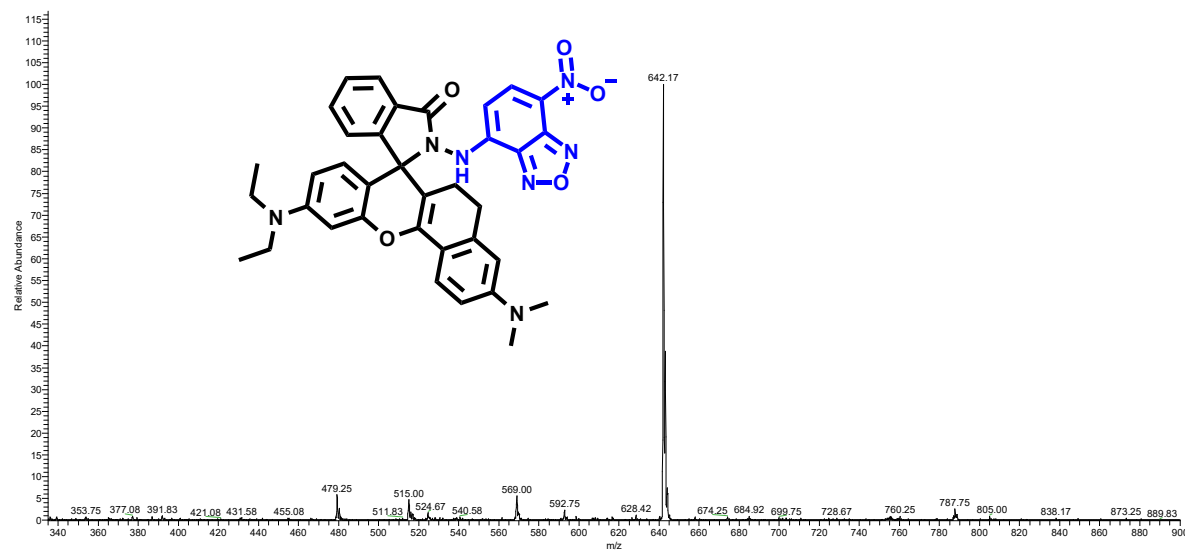


Figure S6. ¹³C NMR spectrum of probe A in CDCl_3 .

probe 3 again_240926225958 #1 RT: 0.00 AV: 1 NL: 6.26E2
T: ITMS - p ESI Full ms [100.00-900.00]



probe 3 again_240926225958 #1 RT: 0.00 AV: 1 NL: 6.26E2
T: ITMS - p ESI Full ms [100.00-900.00]

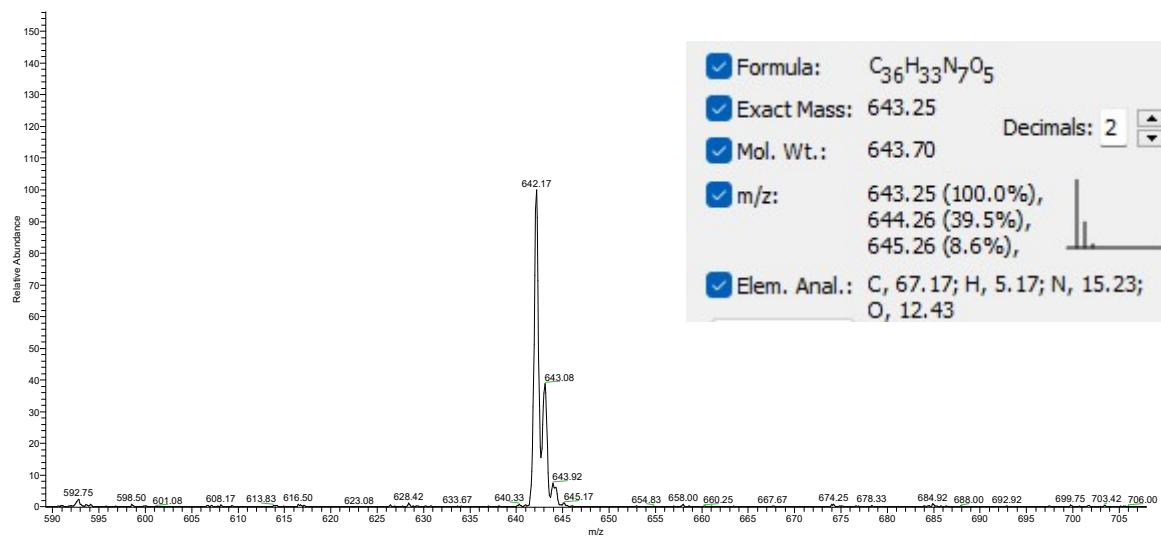


Figure S7. Electrospray ionization (ESI) MS spectrum (top) with expanded region (bottom) probe A.

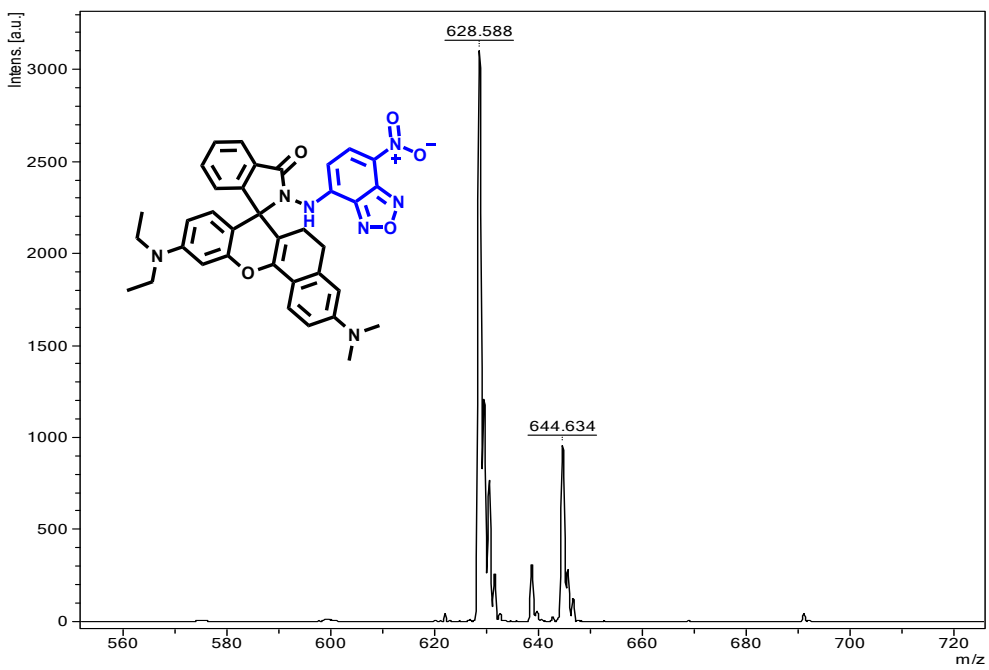


Figure S8. MALDI TOF MS spectrum of probe A.

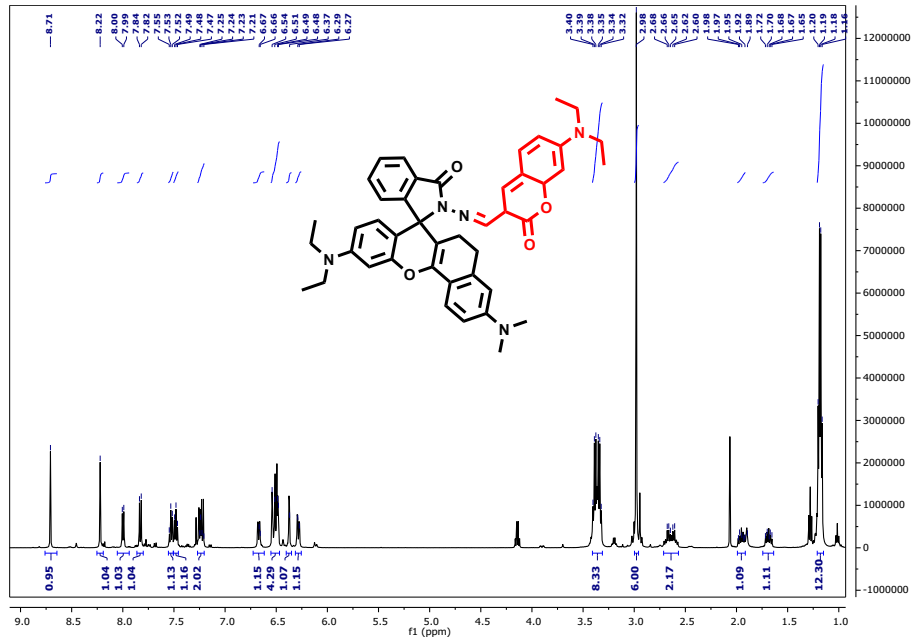


Figure S9. ^1H NMR spectrum of probe B in CDCl_3 .

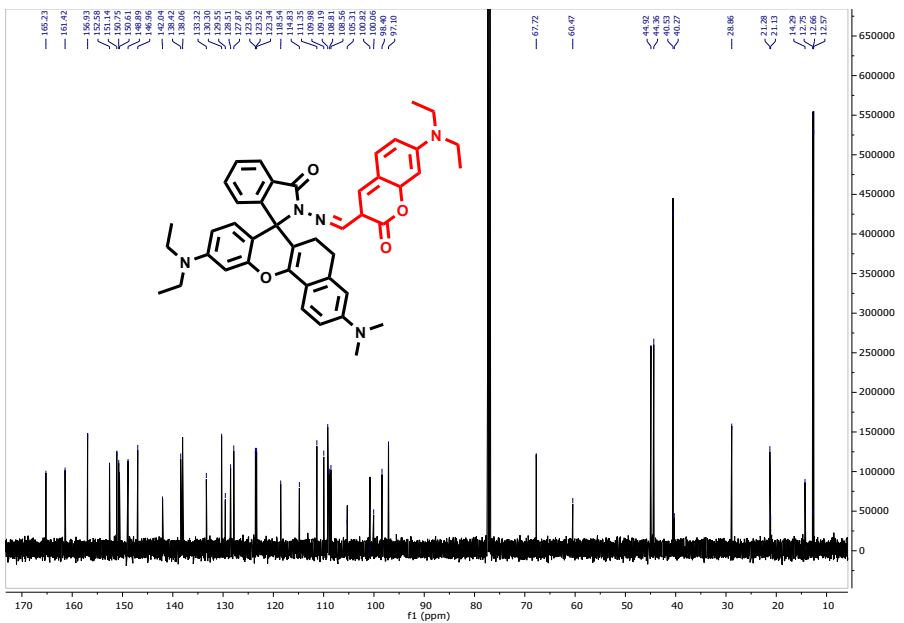


Figure S10. ^{13}C NMR spectrum of probe **B** in CDCl_3 .

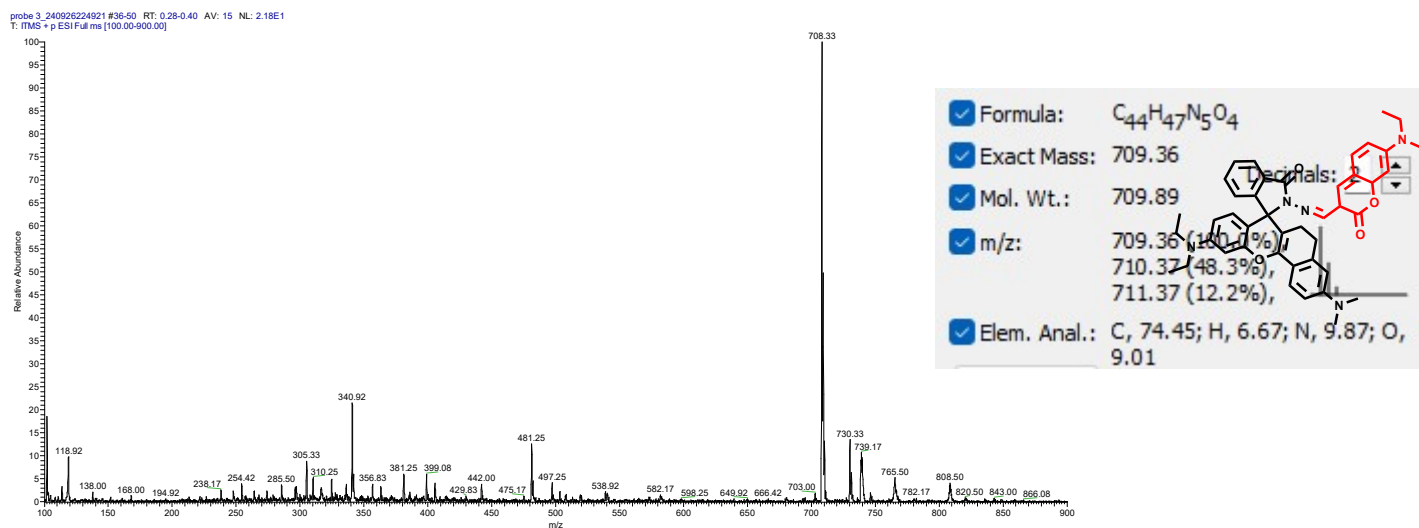


Figure S11. Electrospray ionization (ESI) MS spectrum of probe **B**.

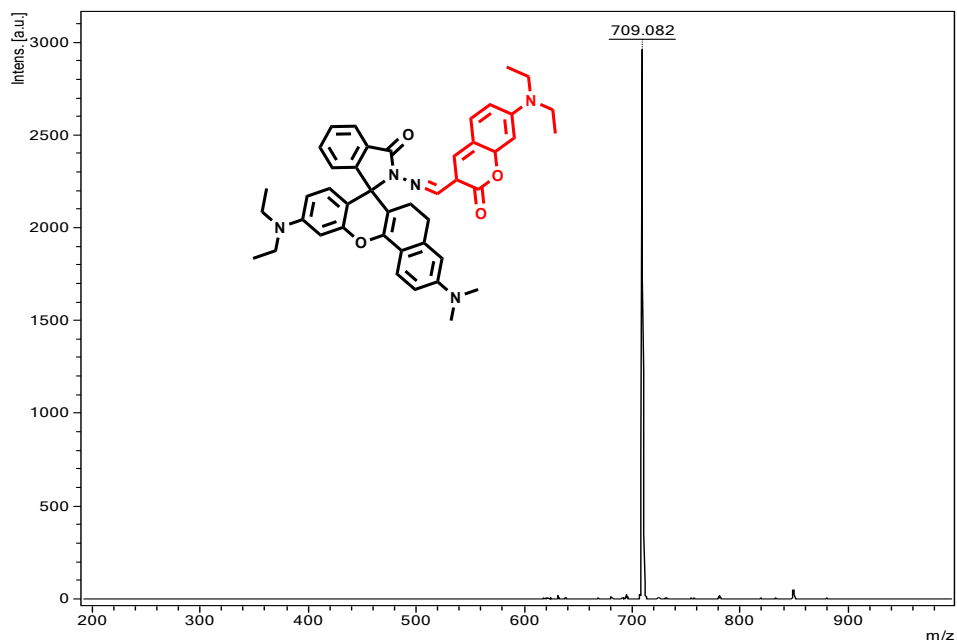


Figure S12. MALDI TOF MS spectrum of probe **B**.

7. FTIR of probes **A** and **B**

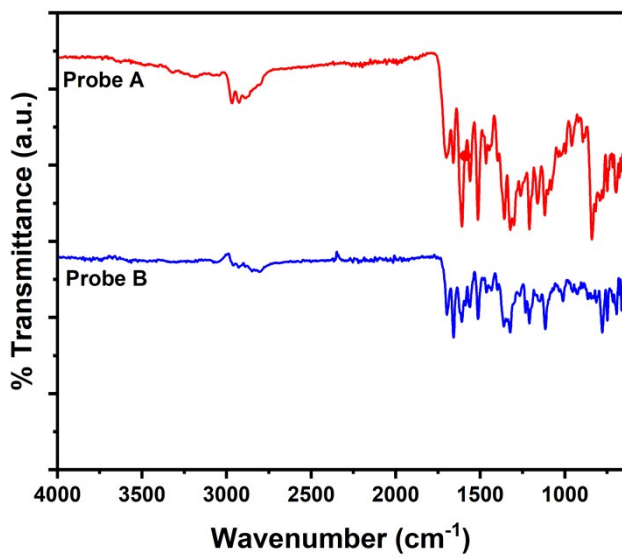


Figure S13. FTIR spectra of probes **A** and **B**.

8. Tauc plot for probe A.

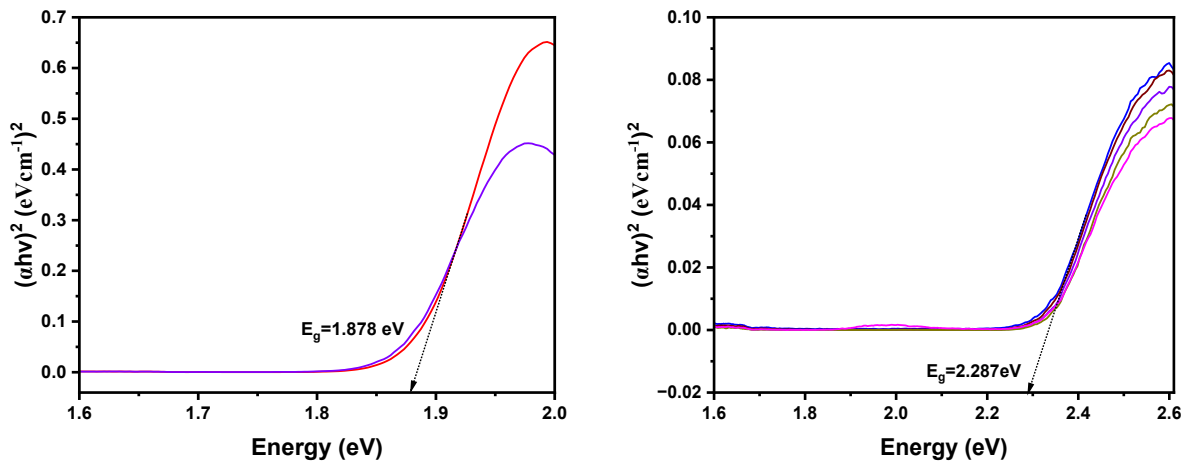


Figure S14. Tauc Plot for probe A under acidic (left) and basic pH (right) conditions.

9. UV-Vis and Fluorescence spectra of probe B

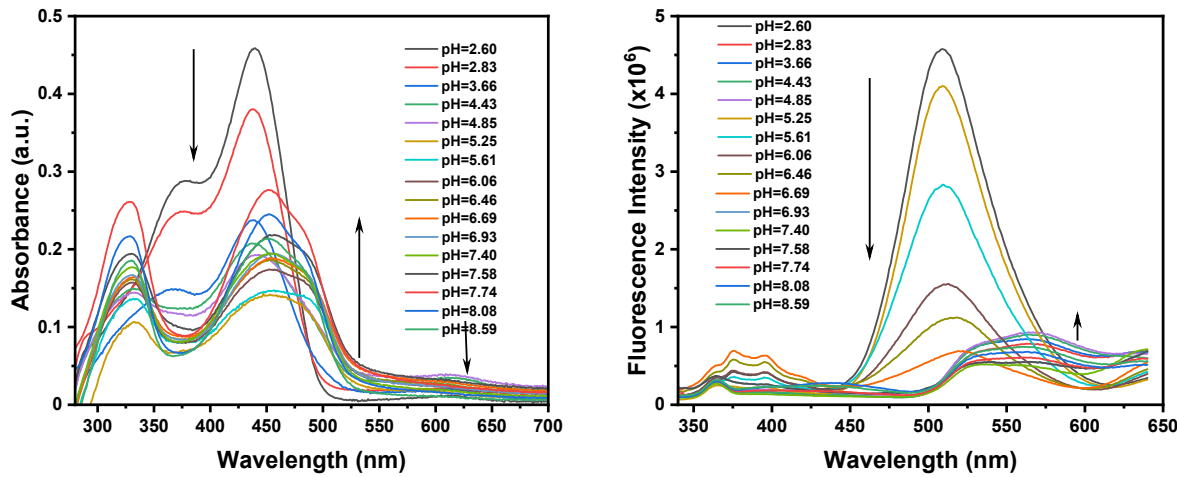
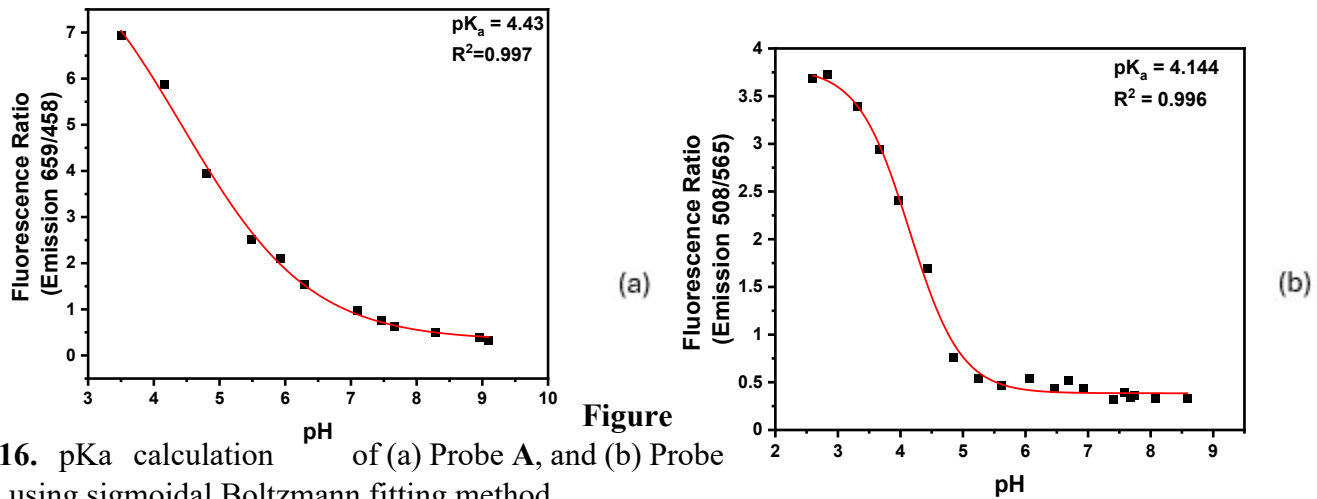


Figure S15. (a) Absorption and (b) fluorescence spectra with excitation at 325 nm of probe B (10 mM) recorded in various pH buffer solutions containing 30% DMSO.

10. Calculation of pKa value of probes **A** and **B**.



11. Selectivity test and Photostability test for probes **A** and **B**

To evaluate the effect of other biological molecules on the pH measurement of probes **A** and **B**, the emission spectra are collected with possible essential cations: Al³⁺, Fe³⁺, Sn²⁺, Na⁺, K⁺, Zn²⁺, Co²⁺, Cu²⁺, Mg²⁺, different classes of anions: PO₄³⁻, acetate, Cl⁻, SO₄²⁻, NO₂⁻, I⁻, SO₃²⁻, CN⁻, NO₃⁻, CO₃²⁻, and various amino acids: glycine, tyrosine, serine, lysine, arginine, cystine, cysteine, glutathione, alanine, valine, and methionine at physiological pH (i.e., 7.4) conditions, Figs. S17 and S18 (a-c). Probes **A** and **B** showed insignificant spectroscopic changes toward the tested anions, cations, and amino acids. These results suggested that probes **A** and **B** have potential as pH-sensitive probes to explore pH-related biological activities as the presence of common cations, anions and amino acids in cells have negligible effects on the pH detection.

The photostability of each probe is examined through emission spectra, Figs. S17 (d) and S18 (d). The emission intensities of probe **A** at 660 nm and probe **B** at 570 nm are recorded for 25 cycles for 125 mins with a 5 min time gap between each cycle. Probe **A** shows very small loss (less than 3% loss in intensity) in relative fluorescence intensity in acidic, neutral and basic pH conditions. Probe **B** displays a photostability of more than 95% in acidic, neutral and basic buffer solutions. It shows that these probes are significantly photostable at different pH conditions for more than 2 hours.

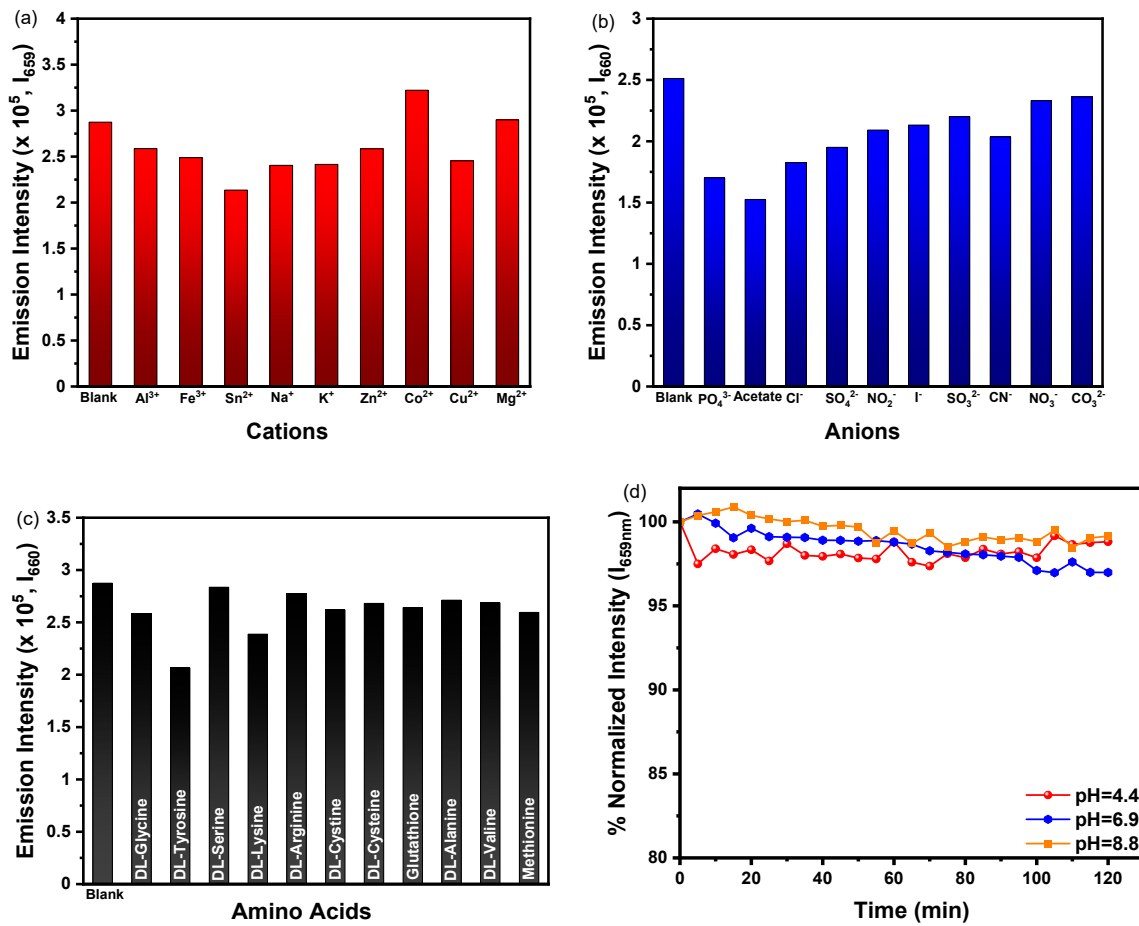


Figure S17. Fluorescence intensity of Probe A in the absence and presence of 50 μM of various (a) metal ions, (b) anions and (c) amino acids. Measurements were taken at pH levels of 7.2 using PBS buffer under excitation at 400 nm. Rhodamine emission peak at 660 nm is used to compare the emission intensity of probe A. (d) Photostability of probe A in acidic, neutral and basic pH for 125 minutes.

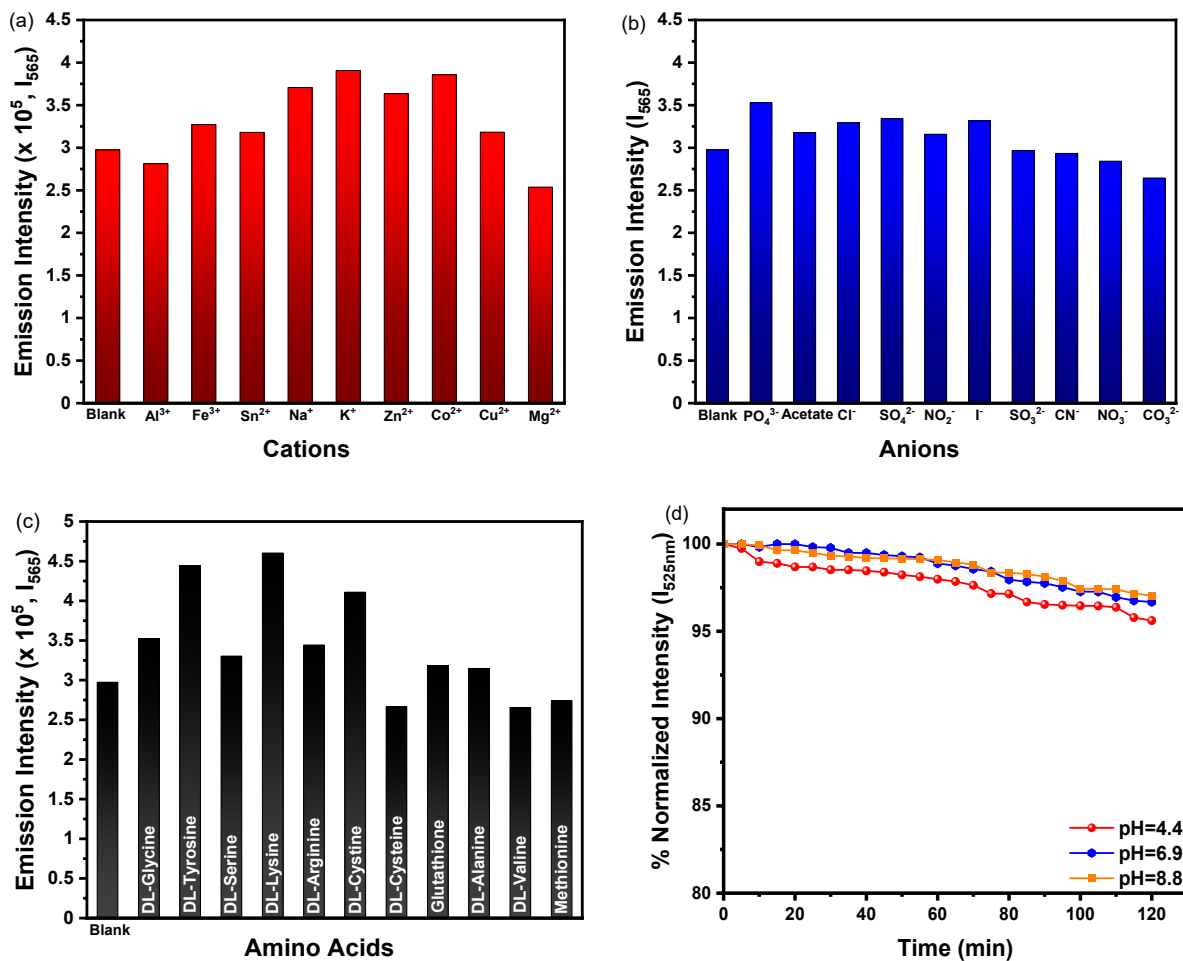


Figure S18. Fluorescence intensity of probe **B** in the absence and presence of 50 μM of various (a) metal ions, (b) anions and (c) amino acids. Measurements were taken at pH levels of 7.2 using PBS buffer under excitation at 380 nm. The emission peak at 570 nm is used to compare the emission intensity of probe **B** in different cations, anions, and amino acids. (d) Photostability of probe **B** in acidic, neutral and basic pH for 125 minutes.

12. Reversibility test for probe A

The reversible fluorescence responses to pH changes for probe **A** are examined with pH varying between 6.93 and 3.30, Fig. S19. The reversibility test is performed for ten cycles. The initial emission intensities were maintained consistently without significant decrease between neutral and acidic cycles.

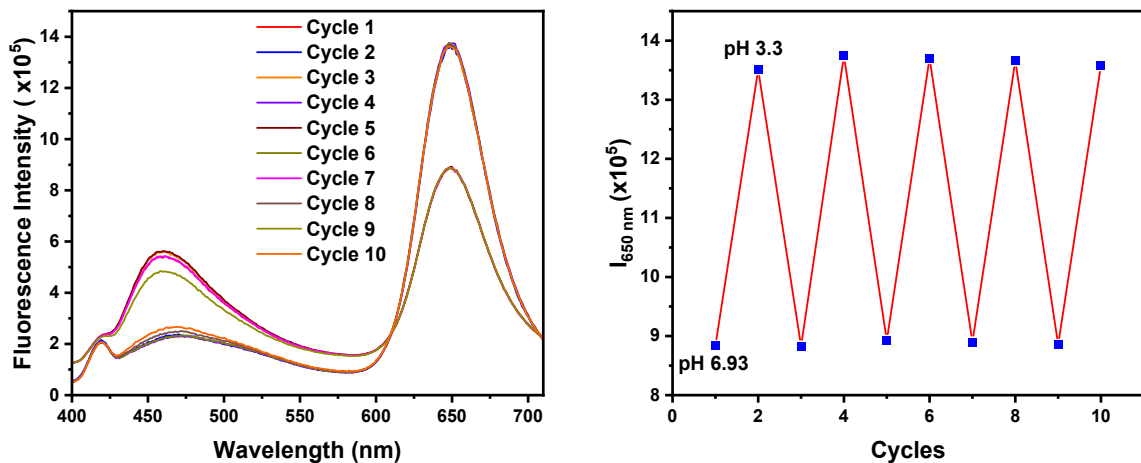


Figure S19. Reversibility test of Probe A between pH 3.3 and 6.93 for 10 cycles.

13. Theoretical Calculations

Optimization and frequency calculations were performed at the APFD/6-311+G(d) level using the Gaussian 16 software suite,² with no imaginary frequencies detected. The first ten excited states were evaluated through TD-DFT optimizations³ in a Polarizable Continuum Model (PCM) of water. Data and figures were interpreted using GaussView 6.⁴ Diagrams and atomic position listings from the calculations are presented sequentially for probes, with all data situated within the water PCM matrix.

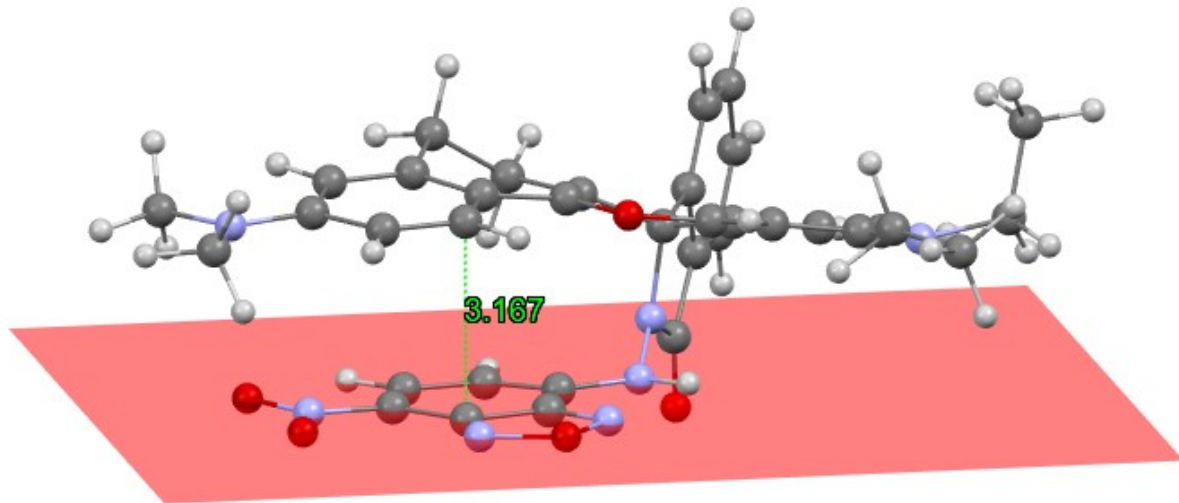


Figure S20. The structure of probe A as displayed in a Mercury⁵ drawing.

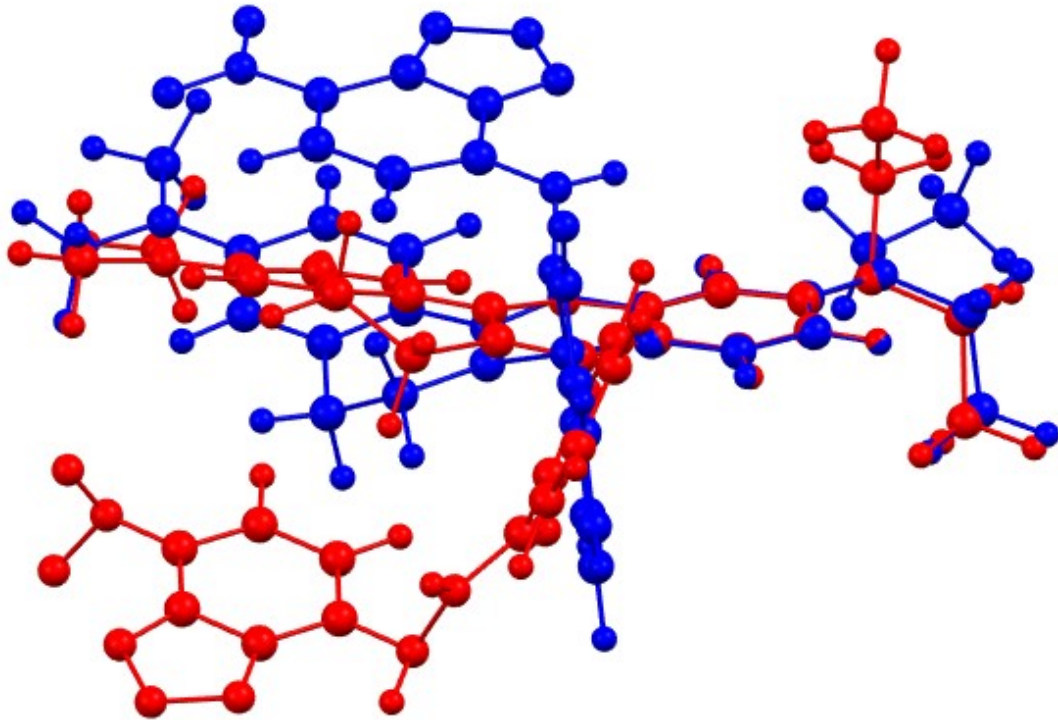


Figure S21. Overlay of the calculated structures for probes **A** (blue) and **AH⁺** (red).

Table S1. Calculated atomic coordinates for probe **A**.

Row	Symbol	X	Y	Z	Row	Symbol	X	Y	Z
1	C	-4.58128	0.622182	-0.1139	16	C	3.415169	1.759525	1.400158
2	C	-4.03589	1.906611	0.147386	17	C	4.321123	0.714093	1.688142
3	C	-2.67523	1.960574	0.495297	18	C	3.778858	-0.57336	1.921291
4	C	-1.90742	0.803548	0.526799	19	N	-1.15642	-1.89962	-1.26726
5	C	-2.43251	-0.45385	0.24879	20	C	-1.65917	-3.063	-1.79849
6	C	-3.79306	-0.50821	-0.071	21	C	-2.27718	-3.75616	-0.64646
7	C	-0.5938	0.982133	0.854746	22	C	-2.20297	-2.95345	0.485474
8	C	0.173222	-0.11633	1.110663	23	C	-2.87673	-5.0085	-0.61462
9	C	-0.25796	-1.38813	0.943133	24	C	-3.40483	-5.44487	0.596078
10	C	-1.52072	-1.64466	0.181828	25	C	-3.32977	-4.63839	1.737205
11	C	1.547128	0.218505	1.438583	26	C	-2.72793	-3.38199	1.693802
12	C	2.424105	-0.81745	1.80672	27	N	-4.80082	3.049666	0.047389
13	C	1.821878	-2.15011	2.152613	28	C	-4.19553	4.310201	0.474032
14	C	0.668236	-2.53317	1.228017	29	C	-5.00683	5.550644	0.136722
15	C	2.06194	1.506118	1.271947	30	C	-6.2529	2.937478	0.118719

Row	Symbol	X	Y	Z	Row	Symbol	X	Y	Z
31	C	-6.77442	2.664381	1.526682	57	H	1.39505	2.317907	1.0022
32	N	5.665954	0.934948	1.735789	58	H	3.774733	2.76688	1.234569
33	C	6.57595	-0.15937	1.99152	59	H	4.427299	-1.39546	2.200348
34	C	6.189173	2.278892	1.610918	60	H	-2.9283	-5.61947	-1.50994
35	O	-1.58385	-3.41634	-2.96146	61	H	-3.88045	-6.41824	0.659413
36	N	-0.67519	-0.86904	-2.01788	62	H	-3.74924	-4.99817	2.671585
37	C	0.655067	-0.56496	-1.92316	63	H	-2.67294	-2.75635	2.579061
38	C	1.660956	-1.49776	-1.76603	64	H	-3.22925	4.394877	-0.03092
39	C	2.999936	-1.10805	-1.59723	65	H	-3.98508	4.287556	1.555258
40	C	3.41959	0.203701	-1.64237	66	H	-5.24741	5.595312	-0.92951
41	C	2.435826	1.204899	-1.87156	67	H	-4.41058	6.433385	0.382135
42	C	1.069924	0.801472	-2.00393	68	H	-5.93677	5.617684	0.706668
43	N	2.478541	2.515554	-1.96391	69	H	-6.58207	2.162052	-0.57513
44	O	1.182764	2.895825	-2.13477	70	H	-6.67865	3.862625	-0.26944
45	N	0.3253	1.866815	-2.15717	71	H	-7.86565	2.587739	1.524911
46	N	4.796297	0.527821	-1.4567	72	H	-6.49344	3.471026	2.210566
47	O	5.585953	-0.3794	-1.21351	73	H	-6.3678	1.728855	1.921609
48	O	5.118227	1.707191	-1.55732	74	H	6.459554	-0.56812	3.003806
49	H	-1.31599	-0.08508	-2.09772	75	H	7.598523	0.199007	1.886882
50	H	-5.62887	0.5071	-0.35696	76	H	6.427582	-0.96732	1.268171
51	H	-2.1795	2.886185	0.752759	77	H	5.939757	2.715562	0.638599
52	H	-4.24282	-1.47189	-0.29152	78	H	5.806526	2.93781	2.400276
53	H	2.584676	-2.93321	2.155837	79	H	7.273751	2.244784	1.696679
54	H	1.438195	-2.08055	3.180185	80	H	1.410982	-2.55024	-1.74285
55	H	1.059773	-2.92587	0.280204	81	H	3.749292	-1.87269	-1.4291
56	H	0.104651	-3.35824	1.675515					

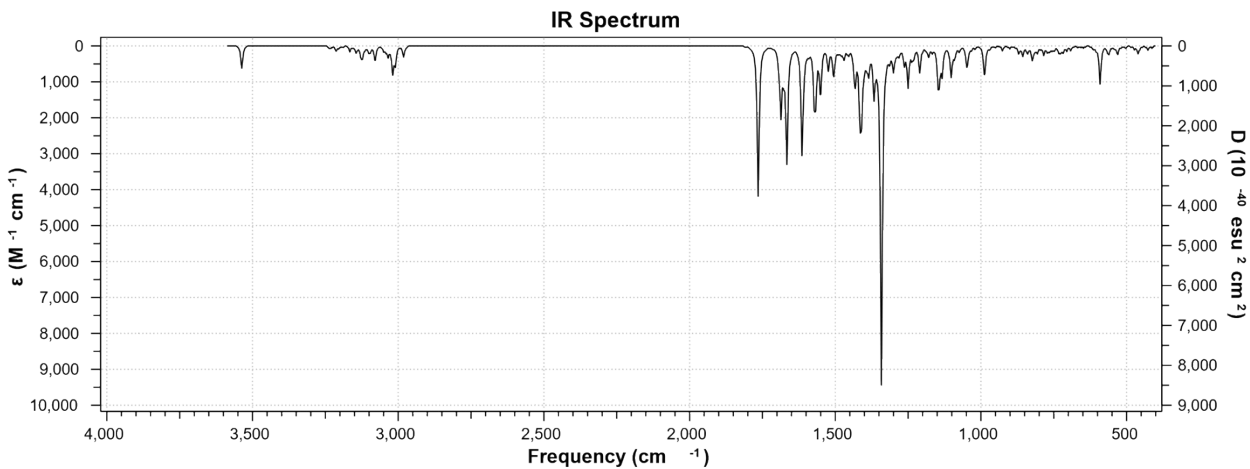


Figure S22. Calculated vibrational spectrum for probe A.

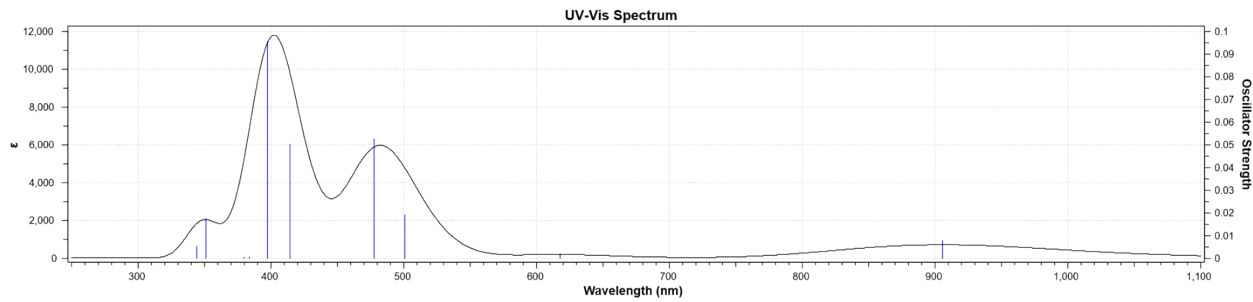


Figure S23. Calculated UV-Vis spectrum for probe A.

Table S2. Excitation energies and oscillator strengths listing for probe A.

Excited State	Nature	E(eV)	$\lambda(\text{nm})$	f	Orbital Transitions	Normalized Coefficient
1	A	1.3689	905.69	0.0078	169 -> 170	0.7043
2	A	2.0072	617.69	0.002	168 -> 170	0.7034
3	A	2.4759	500.76	0.0191	167 -> 170 169 -> 171	0.42045 0.56107
4	A	2.5956	477.67	0.0526	167 -> 170 169 -> 171	0.56005 -0.42054
5	A	2.9917	414.42	0.0503	165 -> 170 166 -> 170	-0.47819 0.50821
6	A	3.1199	397.4	0.0956	165 -> 170 166 -> 170	0.51476 0.47091
7	A	3.2307	383.77	0.0006	169 -> 172	0.69666
8	A	3.2648	379.76	0.0004	168 -> 171	0.69797
9	A	3.5317	351.06	0.0176	164 -> 170	0.67929

Excited State	Nature	E(eV)	$\lambda(\text{nm})$	f	Orbital Transitions	Normalized Coefficient
10	A	3.6026	344.15	0.0052	167 -> 171 168 -> 172	-0.15474 0.6946

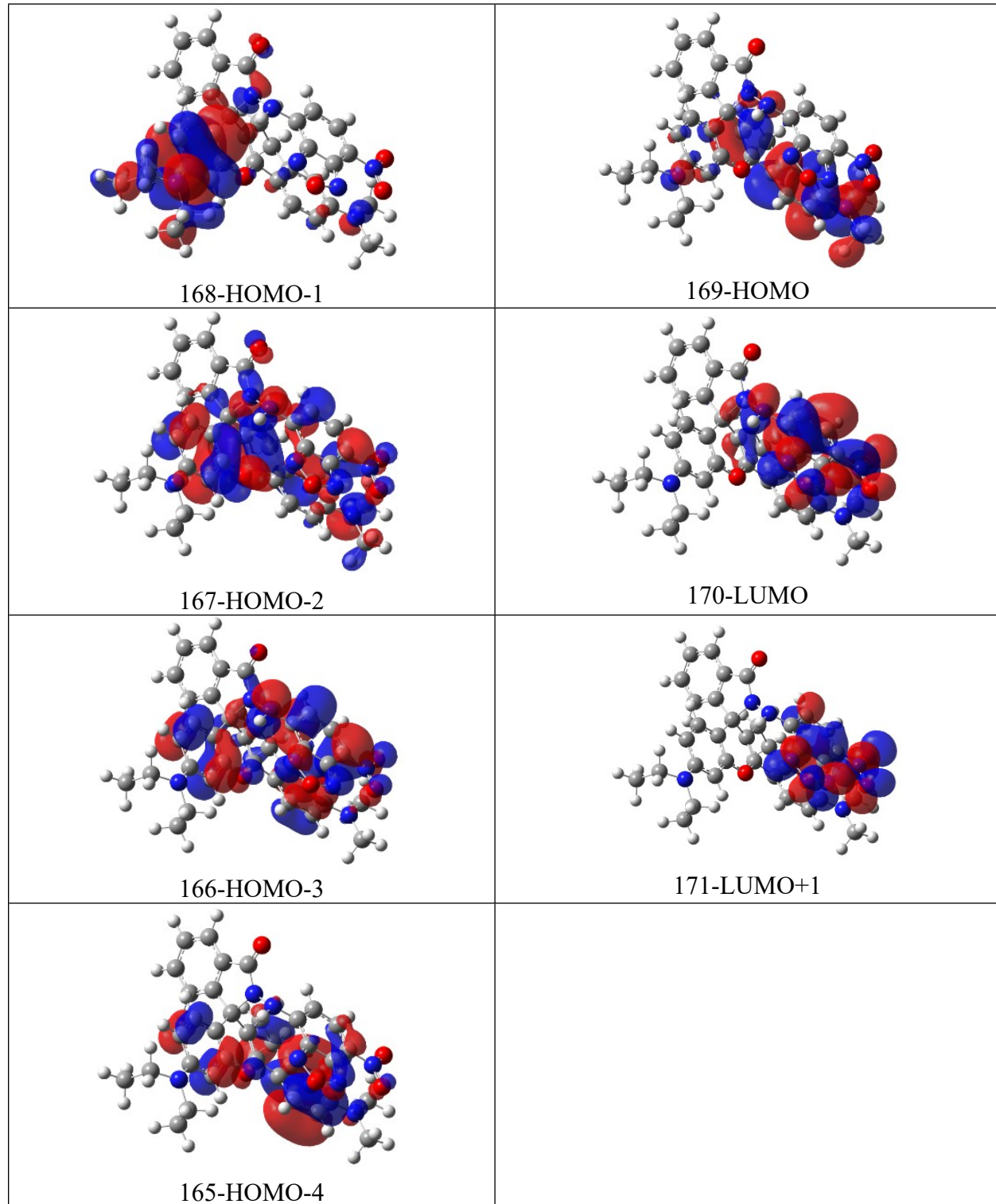


Figure S24. LCAOs for probe **A** involved with the transition noted as Excited States 1, 4, and 6 in Table S2.

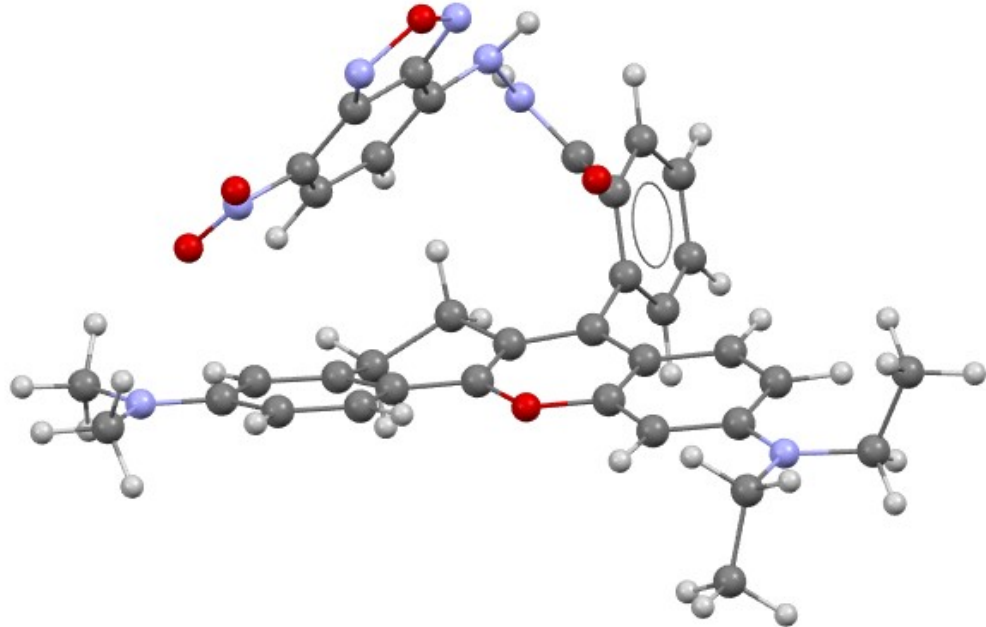


Figure S25. Mercury⁵ representation of probe AH⁺.

Table S3. Calculated atomic coordinates for probe AH⁺.

Row	Symbol	X	Y	Z	Row	Symbol	X	Y	Z
1	C	-4.88096	-0.72202	0.030605	17	C	3.889436	-1.38952	2.279234
2	C	-4.33907	-2.04703	-0.03223	18	C	3.32368	-0.17795	2.76175
3	C	-2.99353	-2.22218	0.359418	19	N	0.014687	3.454267	-1.30831
4	C	-2.26836	-1.1387	0.796506	20	C	-1.09796	2.763119	-0.90021
5	C	-2.79531	0.166318	0.88634	21	C	-1.8949	3.408988	0.183752
6	C	-4.13284	0.335387	0.465371	22	C	-2.36935	2.61551	1.24166
7	O	-0.9699	-1.36694	1.126774	23	C	-2.23274	4.759635	0.123443
8	C	-0.18069	-0.39455	1.593243	24	C	-3.04206	5.322123	1.105879
9	C	-0.65823	0.908909	1.757106	25	C	-3.5104	4.536734	2.152989
10	C	-1.94532	1.19824	1.325342	26	C	-3.1724	3.187033	2.222351
11	C	1.171797	-0.76019	1.830294	27	N	-5.08794	-3.08501	-0.4632
12	C	1.998035	0.130094	2.556328	28	C	-4.52604	-4.42071	-0.62549
13	C	1.369201	1.347487	3.172624	29	C	-4.57008	-5.23977	0.659978
14	C	0.2856	1.954579	2.285642	30	C	-6.50242	-2.94469	-0.79236
15	C	1.72308	-1.96407	1.346188	31	C	-6.73359	-2.54217	-2.24428
16	C	3.039805	-2.27728	1.559701	32	N	5.185989	-1.68875	2.494232

Row	Symbol	X	Y	Z	Row	Symbol	X	Y	Z
33	C	6.065799	-0.7336	3.14192	58	H	3.433967	-3.19854	1.152363
34	C	5.730911	-2.96756	2.072309	59	H	3.929327	0.514761	3.332716
35	O	-1.38813	1.687495	-1.39185	60	H	0.27521	4.357048	-0.93821
36	N	0.739601	2.966158	-2.36381	61	H	-1.89221	5.36887	-0.70807
37	C	1.609419	1.941922	-2.15466	62	H	-3.31076	6.371489	1.046928
38	C	2.187009	1.624699	-0.9404	63	H	-4.14101	4.972494	2.921033
39	C	3.120544	0.580674	-0.81749	64	H	-3.52368	2.574662	3.046447
40	C	3.510788	-0.21062	-1.87318	65	H	-5.10081	-4.91682	-1.4116
41	C	2.933345	0.051104	-3.14676	66	H	-3.50574	-4.33829	-1.0082
42	C	2.00614	1.132919	-3.26867	67	H	-3.99466	-4.76096	1.456585
43	N	3.069067	-0.49803	-4.3337	68	H	-5.59945	-5.35804	1.009829
44	O	2.254413	0.224072	-5.14757	69	H	-4.15316	-6.23594	0.488409
45	N	1.606835	1.209968	-4.51255	70	H	-6.97371	-3.90911	-0.58621
46	N	4.483261	-1.23996	-1.68539	71	H	-6.96674	-2.2345	-0.10485
47	O	4.665646	-2.02117	-2.61313	72	H	-6.30037	-3.2795	-2.92596
48	O	5.081081	-1.28853	-0.6165	73	H	-7.8049	-2.4754	-2.45303
49	H	0.268516	3.000662	-3.25995	74	H	-6.28074	-1.57168	-2.46395
50	H	-5.89755	-0.53957	-0.29059	75	H	7.081291	-1.12239	3.125863
51	H	-2.50604	-3.18696	0.336281	76	H	5.779539	-0.56401	4.185716
52	H	-4.56623	1.329397	0.487348	77	H	6.059971	0.22562	2.615318
53	H	0.918375	1.043075	4.126804	78	H	6.761211	-3.03937	2.413416
54	H	2.130055	2.094694	3.409127	79	H	5.169384	-3.79734	2.512074
55	H	-0.2805	2.702939	2.845857	80	H	5.71729	-3.06191	0.982889
56	H	0.741329	2.496328	1.448862	81	H	1.9414	2.207316	-0.06418
57	H	1.098693	-2.64354	0.776541	82	H	3.557197	0.38747	0.156287

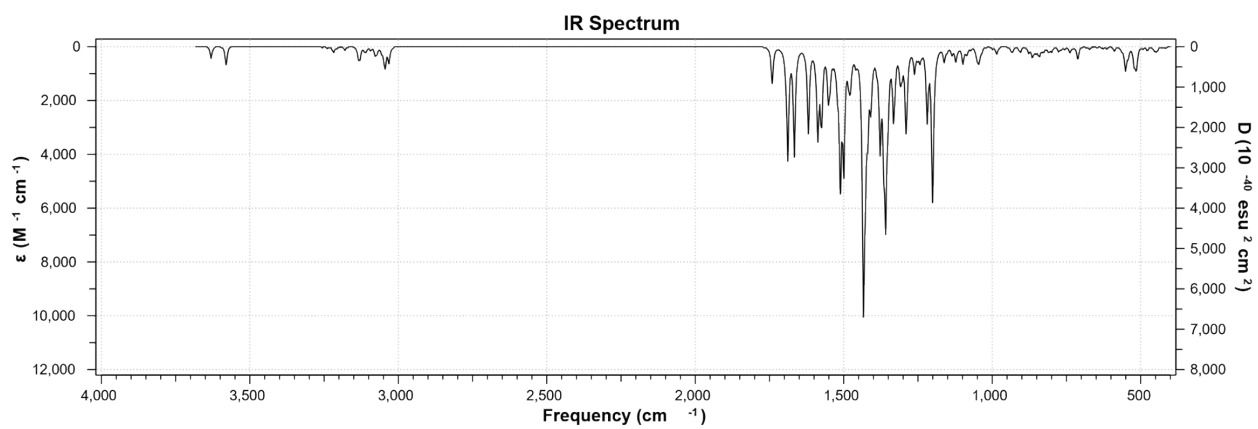


Figure S26. Calculated vibrational spectrum for probe AH^+ .

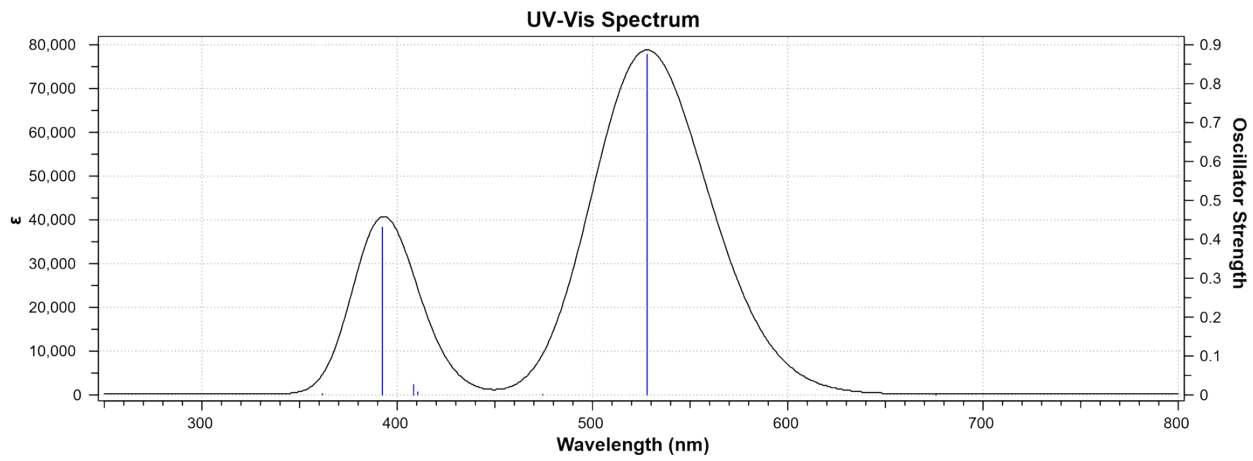


Figure S27. Calculated UV-Vis spectrum for probe AH^+ .

Table S4. Excitation energies and oscillator strengths listing for probe AH^+ .

Excited State	Nature	E(eV)	$\lambda(\text{nm})$	f	Orbital Transitions	Normalized Coefficient
1	A	1.8343	675.93	0.0005	$169 \rightarrow 170$	0.7009
2	A	2.3482	528	0.875	$169 \rightarrow 171$	0.7004
3	A	2.6131	474.48	0.0012	$168 \rightarrow 170$	0.6956
4	A	3.0198	410.57	0.0074	$167 \rightarrow 170$	-0.13493
					$168 \rightarrow 171$	-0.1888
					$169 \rightarrow 172$	0.65459
5	A	3.0361	408.37	0.026	$167 \rightarrow 170$	0.20755
					$168 \rightarrow 171$	0.62084
					$169 \rightarrow 172$	0.2244
6	A	3.1596	392.4	0.4307	$167 \rightarrow 170$	0.64847
					$168 \rightarrow 171$	-0.2245
7	A	3.428	361.68	0.0029	$167 \rightarrow 171$	0.70603

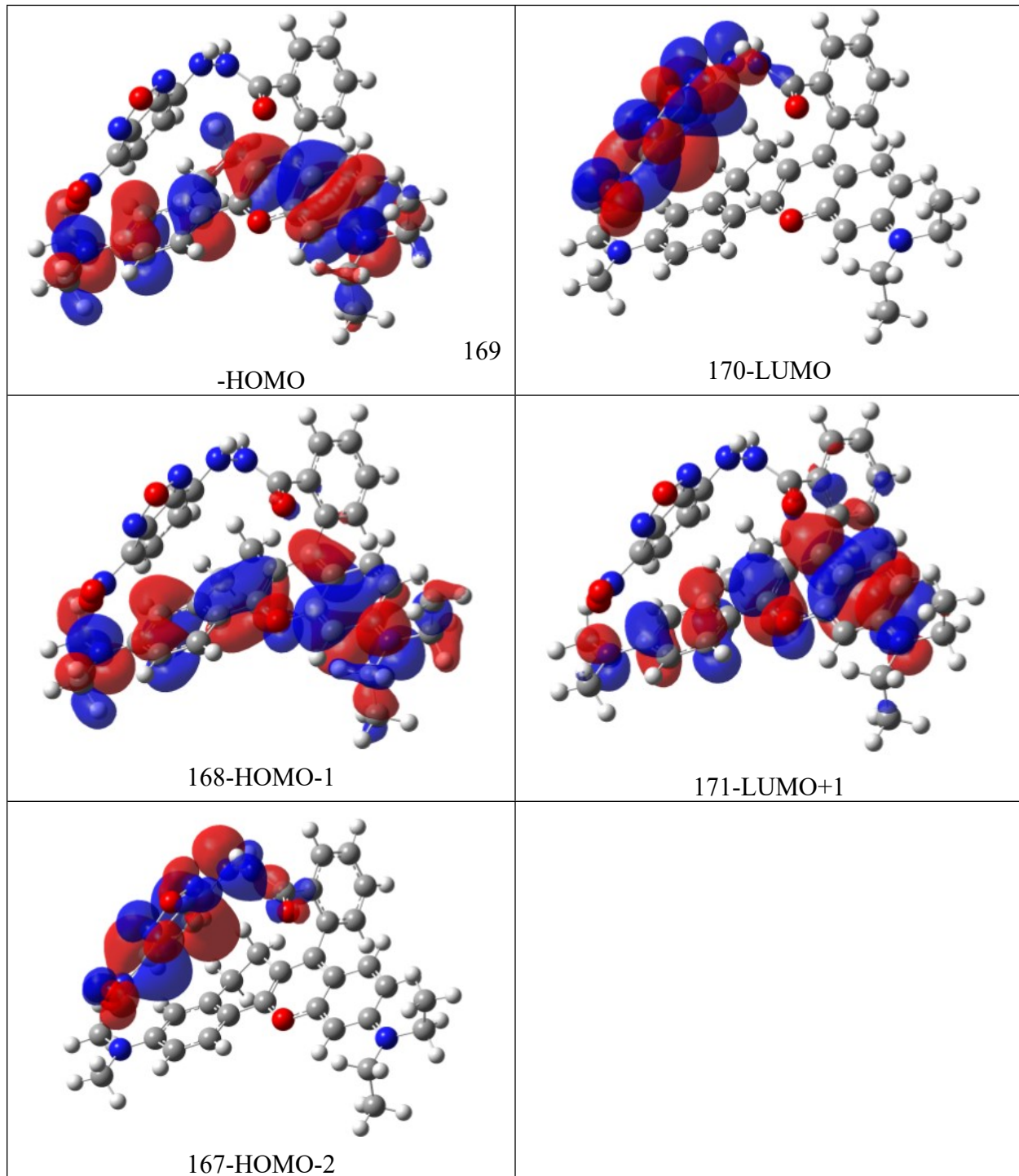


Figure S28. LCAOs for probe AH^+ involved with the transition noted as Excited States 1, 2 and 6 in Table S4.

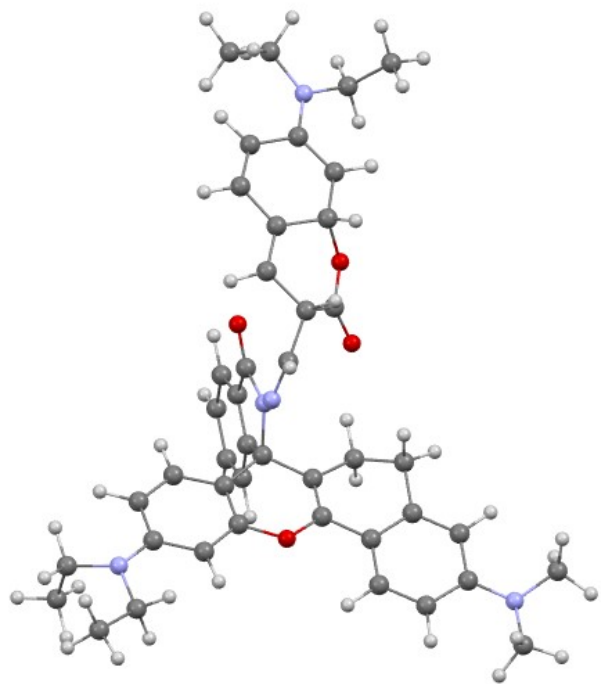


Figure S29. The structure of probe **B** as displayed in a Mercury⁵ drawing.

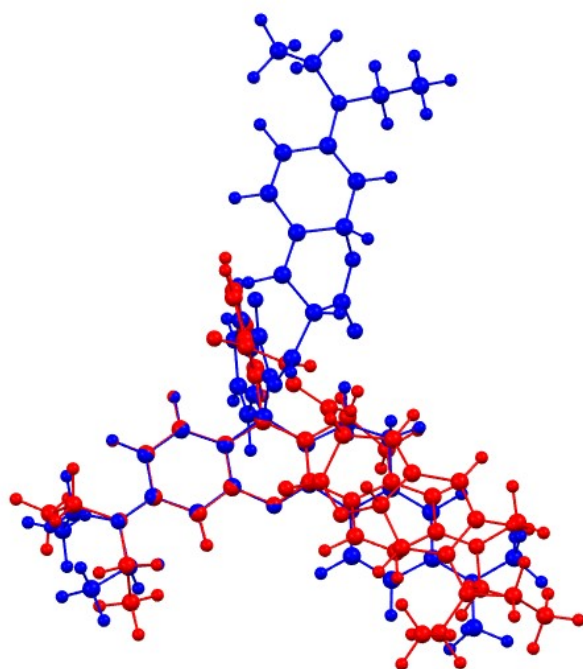


Figure S30. Overlay of the calculated structures for probes **B** (blue) and BH^+ (red).

Table S5. Calculated atomic coordinates for probe **B**.

Row	Symbol	X	Y	Z	Row	Symbol	X	Y	Z
1	C	-2.83562	-3.93083	0.053123	40	C	3.863745	1.268175	-0.34209
2	C	-3.99894	-3.56261	-0.67017	41	C	4.861991	0.805963	-1.35914
3	C	-4.26116	-2.18869	-0.79397	42	C	4.524444	-0.59654	-1.77931
4	C	-3.38599	-1.24526	-0.26412	43	C	3.235536	-0.84776	-2.03437
5	C	-2.23578	-1.6035	0.426479	44	C	6.221667	0.996335	-0.81235
6	C	-1.99188	-2.97132	0.572734	45	C	7.145497	-0.00933	-0.77037
7	C	-3.74974	0.056671	-0.45953	46	C	6.783852	-1.34037	-1.28061
8	C	-3.00488	1.034242	0.139419	47	C	5.556849	-1.60329	-1.76119
9	C	-1.86919	0.80851	0.822269	48	N	8.406431	0.151348	-0.25704
10	C	-1.27804	-0.56082	0.932451	49	C	9.481654	-0.81303	-0.44577
11	C	-3.5792	2.366452	-0.00474	50	C	9.608875	-1.805	0.705934
12	C	-2.77395	3.480833	0.291576	51	C	8.779099	1.387059	0.406059
13	C	-1.33442	3.241383	0.662245	52	C	9.302845	2.459212	-0.54797
14	C	-1.1693	1.965659	1.480651	53	O	1.727965	1.681013	0.036879
15	C	-4.89159	2.583253	-0.42944	54	H	-2.58831	-4.97226	0.209227
16	C	-5.41066	3.862836	-0.54435	55	H	-5.14438	-1.8124	-1.29177
17	C	-4.62564	4.992013	-0.22351	56	H	-1.10481	-3.29031	1.11356
18	C	-3.29072	4.760677	0.181141	57	H	-0.74885	3.136681	-0.26199
19	N	0.011325	-0.61776	0.167897	58	H	-0.92796	4.104356	1.197651
20	C	1.073681	-1.07945	0.908266	59	H	-0.10687	1.735291	1.58613
21	C	0.574917	-1.17992	2.292033	60	H	-1.5697	2.109919	2.495305
22	C	-0.77536	-0.86739	2.320718	61	H	-5.51961	1.73306	-0.67461
23	C	1.271998	-1.5216	3.444278	62	H	-6.43245	3.982104	-0.88204
24	C	0.568889	-1.5331	4.644675	63	H	-2.63843	5.595551	0.409292
25	C	-0.79373	-1.21203	4.676129	64	H	2.328467	-1.76605	3.401592
26	C	-1.48213	-0.87534	3.511787	65	H	1.078299	-1.79124	5.567641
27	N	-4.82531	-4.51362	-1.24197	66	H	-1.32154	-1.22723	5.624761
28	C	-6.07451	-4.04807	-1.84011	67	H	-2.53941	-0.63001	3.535105
29	C	-6.82929	-5.10331	-2.63279	68	H	-5.82366	-3.23198	-2.52332
30	C	-4.80417	-5.87083	-0.70881	69	H	-6.73601	-3.62023	-1.06923
31	C	-5.48712	-6.00501	0.649587	70	H	-6.19204	-5.56548	-3.39256
32	N	-5.13894	6.264551	-0.29132	71	H	-7.66653	-4.62244	-3.14552
33	C	-4.24856	7.401042	-0.18391	72	H	-7.24504	-5.89221	-2.00112
34	C	-6.42796	6.480381	-0.91365	73	H	-3.76974	-6.21487	-0.65793
35	O	2.179645	-1.37196	0.478226	74	H	-5.28296	-6.52372	-1.43874
36	N	-0.11272	-0.53183	-1.17349	75	H	-5.44178	-7.03913	1.003603
37	C	0.812411	-0.1823	-1.98109	76	H	-6.54055	-5.71516	0.588191
38	C	2.245636	0.268181	-1.8497	77	H	-5.00366	-5.36791	1.395873
39	C	2.571647	1.118482	-0.62484	78	H	-3.51017	7.43439	-0.99762

Row	Symbol	X	Y	Z
79	H	-4.83822	8.316076	-0.21761
80	H	-3.70999	7.389929	0.767698
81	H	-6.69186	7.533174	-0.82407
82	H	-6.43034	6.211513	-1.97963
83	H	-7.20746	5.90037	-0.41211
84	H	0.474427	-0.2222	-3.01672
85	H	2.398699	0.974065	-2.68929
86	H	4.687378	1.495781	-2.19908
87	H	2.875138	-1.8337	-2.30479
88	H	6.47644	2.008138	-0.52493
89	H	7.510702	-2.14083	-1.23301

Row	Symbol	X	Y	Z
90	H	5.29792	-2.60561	-2.09053
91	H	10.41191	-0.24569	-0.5513
92	H	9.352773	-1.33323	-1.39735
93	H	8.705521	-2.41344	0.805228
94	H	9.766625	-1.28213	1.653902
95	H	10.45835	-2.47581	0.544778
96	H	7.914826	1.755318	0.967158
97	H	9.545405	1.144386	1.149081
98	H	8.557746	2.717312	-1.30462
99	H	9.560096	3.368854	0.002798
100	H	10.2031	2.114057	-1.06517

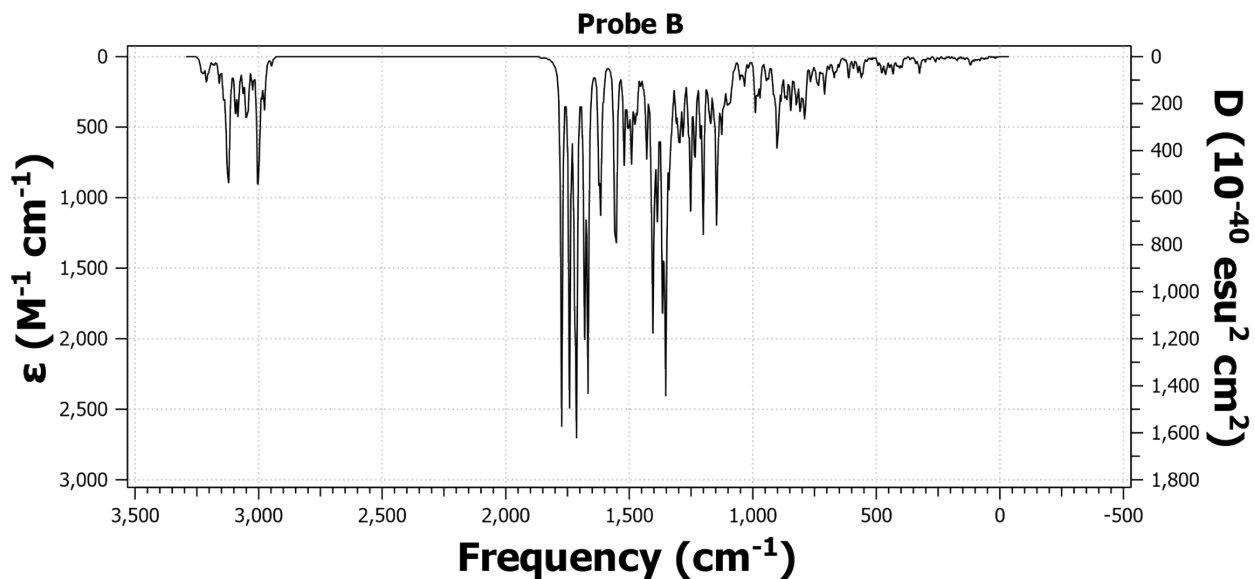


Figure S31. Calculated vibrational spectrum for probe B.

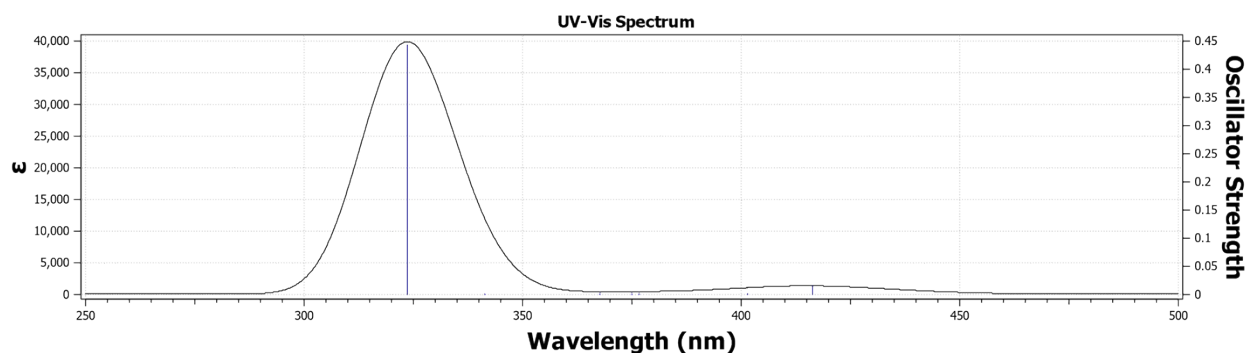


Figure S32. Calculated UV-Vis spectrum for probe **B**.

Table S6. Excitation energies and oscillator strengths listing for probe **B**.

Excited State	Nature	E(eV)	λ (nm)	f	Orbital Transitions	Normalized Coefficient
1	A	2.9778	416.36	0.0136	188->190	0.63889
					188->191	0.29865
2	A	3.0884	401.45	0.0013	189->190	0.56562
					189->191	-0.40999
3	A	3.2919	376.63	0.0012	188->190	-0.29717
					188->191	0.63659
4	A	3.3063	375	0.001	189->190	0.41795
					189->191	0.56545
5	A	3.3722	367.67	0.0011	187->190	0.53997
					187->191	-0.4415
6	A	3.6321	341.36	0.001	187->191	0.44964
					187->192	0.54258
7	A	3.8311	323.63	0.4429	189->192	0.69443

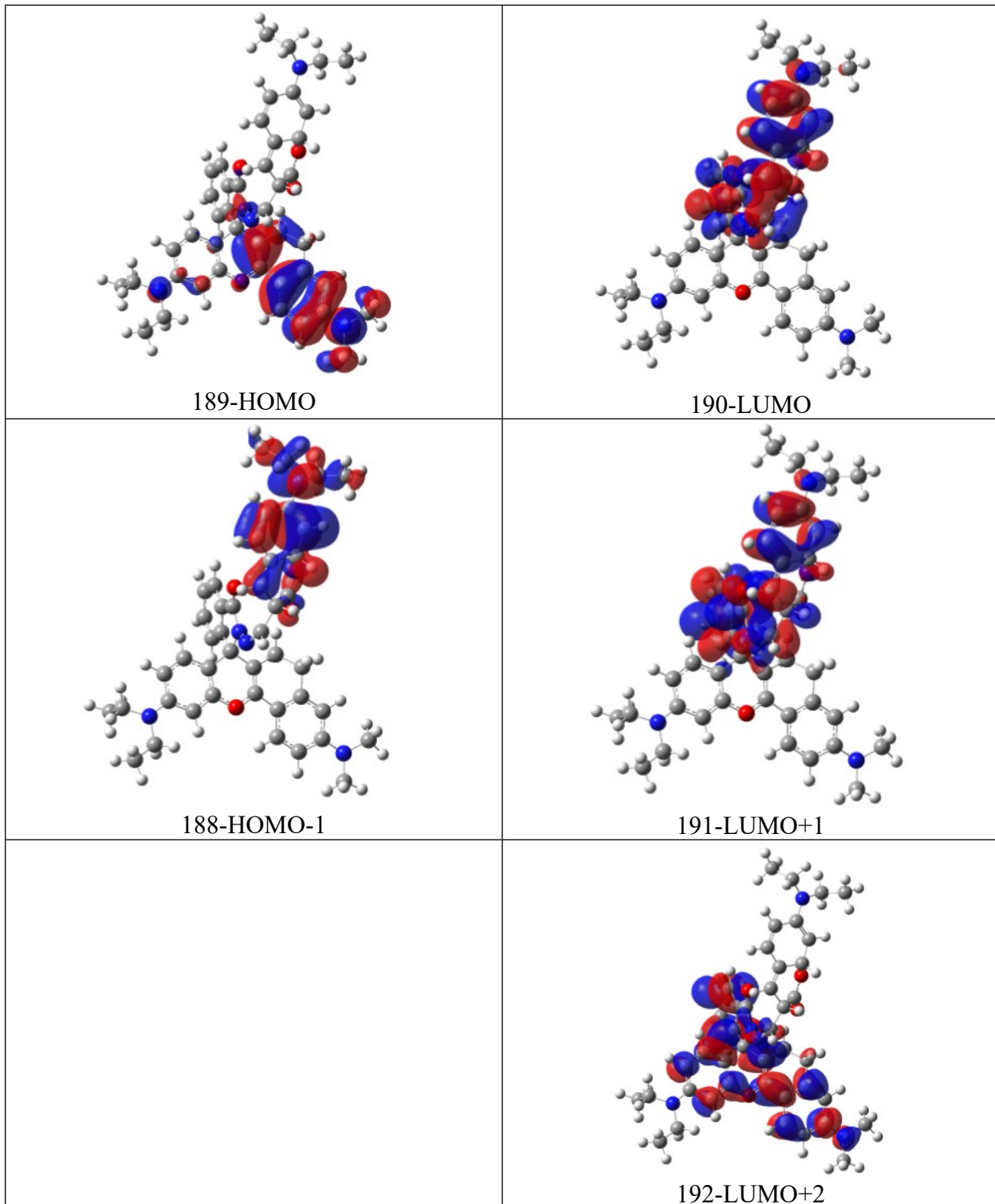


Figure S33. LCAOs for probe **B** involved with the transition noted as Excited States 1 and 7 in Table S10.

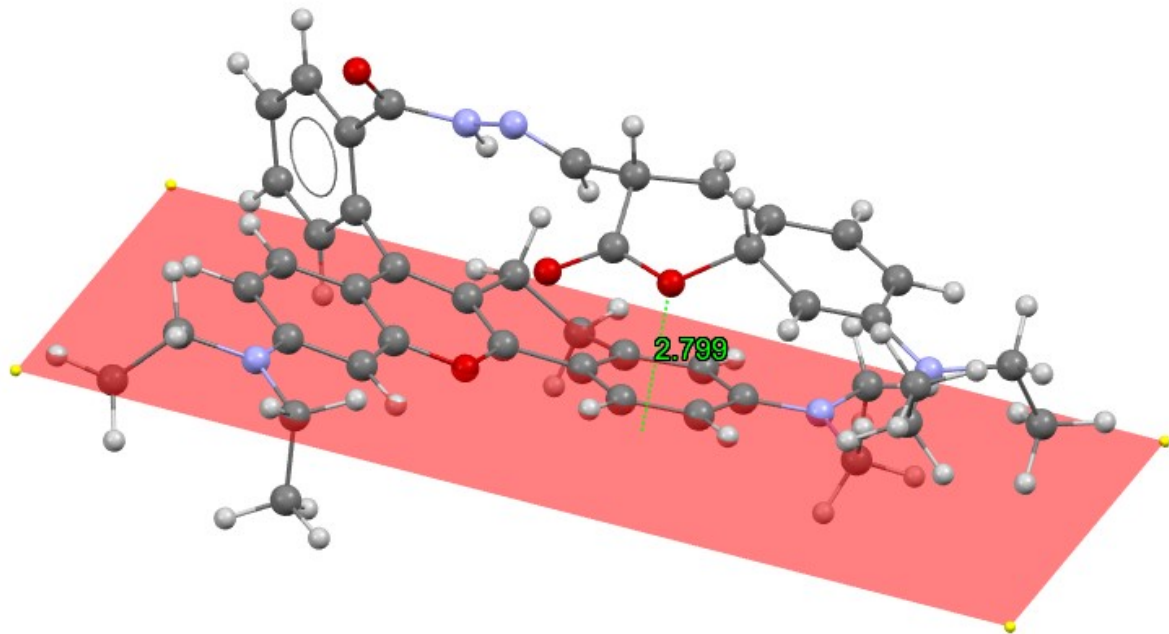


Figure S34. Mercury⁵ representation of probe BH^+ .

Table S7. Calculated atomic coordinates for probe BH^+ .

Row	Symbol	X	Y	Z	Row	Symbol	X	Y	Z
1	C	5.15628	-1.87155	-0.04666	20	C	3.72658	1.721129	-2.24168
2	C	4.175461	-2.8464	0.32587	21	C	4.543643	2.483716	-1.23773
3	C	2.937373	-2.37044	0.808806	22	C	4.285981	2.334775	0.136518
4	C	2.707801	-1.01725	0.87315	23	C	5.558486	3.331417	-1.67204
5	C	3.654657	-0.04363	0.492786	24	C	6.30047	4.058614	-0.7484
6	C	4.898855	-0.53187	0.030879	25	C	6.036997	3.927723	0.612639
7	C	1.49491	-0.62969	1.333607	26	C	5.040905	3.062825	1.054574
8	C	1.137531	0.653843	1.38622	27	N	4.423948	-4.17047	0.205622
9	C	2.054067	1.678617	1.099713	28	C	3.448238	-5.15815	0.656064
10	C	3.305581	1.321674	0.610124	29	C	3.431219	-5.36696	2.16818
11	C	-0.23528	0.885365	1.657961	30	C	5.714334	-4.66578	-0.2654
12	C	-0.67357	2.211635	1.892549	31	C	6.794293	-4.70153	0.811986
13	C	0.373557	3.264043	2.122281	32	N	-4.30196	1.691719	2.075287
14	C	1.570892	3.10405	1.187213	33	C	-4.80918	3.04989	2.055162
15	C	-1.18586	-0.15603	1.626594	34	C	-5.24263	0.614707	2.329863
16	C	-2.52131	0.102437	1.774809	35	O	4.192207	0.990592	-3.09733
17	C	-2.98395	1.435757	1.951189	36	N	1.404344	1.161991	-2.53407
18	C	-2.01709	2.476965	2.010623	37	C	0.286807	1.320173	-1.94719
19	N	2.394472	1.951171	-2.04298	38	C	-0.93344	0.534888	-2.28872

Row	Symbol	X	Y	Z	Row	Symbol	X	Y	Z
39	C	-0.9493	-0.78361	-1.48954	71	H	2.640883	-6.07342	2.437091
40	O	-2.13386	-1.34519	-1.27585	72	H	3.244265	-4.43122	2.701156
41	C	-3.34316	-0.78323	-1.92359	73	H	4.382091	-5.77254	2.520556
42	C	-3.33726	0.716707	-1.8193	74	H	6.035841	-4.06213	-1.1181
43	C	-2.17152	1.338872	-2.0216	75	H	5.54217	-5.67009	-0.65718
44	C	-4.53861	-1.45003	-1.35473	76	H	7.740642	-5.03906	0.379915
45	C	-5.65982	-0.75649	-1.01321	77	H	6.526146	-5.38933	1.616979
46	C	-5.6621	0.710834	-1.11732	78	H	6.954912	-3.71306	1.250459
47	C	-4.56539	1.394618	-1.47896	79	H	-4.32477	3.627898	1.265519
48	N	-6.78956	-1.34157	-0.49274	80	H	-5.87645	3.021927	1.84101
49	C	-8.10841	-0.72373	-0.58593	81	H	-4.6588	3.560716	3.013881
50	C	-8.57976	-0.09182	0.718671	82	H	-4.87772	-0.0359	3.129243
51	C	-6.78092	-2.74613	-0.12812	83	H	-5.42752	0.01022	1.437496
52	C	-7.08427	-3.70007	-1.28384	84	H	-6.18699	1.046832	2.65427
53	O	0.056925	-1.29921	-1.06213	85	H	0.16901	2.036331	-1.12765
54	H	6.129222	-2.18897	-0.39587	86	H	-0.89138	0.226999	-3.34664
55	H	2.143056	-3.03341	1.120984	87	H	-3.22141	-1.06828	-2.9803
56	H	5.666653	0.176296	-0.25953	88	H	-2.08814	2.420371	-1.96713
57	H	-0.05201	4.264686	2.020561	89	H	-4.51535	-2.5319	-1.347
58	H	0.717577	3.169326	3.160652	90	H	-6.5494	1.256336	-0.82078
59	H	1.284105	3.471175	0.190108	91	H	-4.56313	2.480478	-1.46978
60	H	2.388012	3.752226	1.510382	92	H	-8.81508	-1.50177	-0.89348
61	H	-0.85459	-1.16881	1.433385	93	H	-8.11572	0.007891	-1.39689
62	H	-3.22852	-0.71294	1.697495	94	H	-7.96387	0.768553	0.990987
63	H	-2.32952	3.494985	2.210289	95	H	-8.53376	-0.81148	1.541277
64	H	2.149618	2.642785	-1.34312	96	H	-9.61549	0.248679	0.625354
65	H	5.750588	3.427249	-2.73579	97	H	-5.80777	-2.97526	0.316896
66	H	7.082443	4.728774	-1.08993	98	H	-7.52275	-2.88178	0.665734
67	H	6.617873	4.490866	1.335839	99	H	-6.3678	-3.58539	-2.10062
68	H	4.861556	2.931069	2.116853	100	H	-7.04413	-4.7372	-0.93819
69	H	3.689066	-6.09528	0.151241	101	H	-8.08509	-3.52334	-1.68849
70	H	2.458098	-4.86546	0.293788					

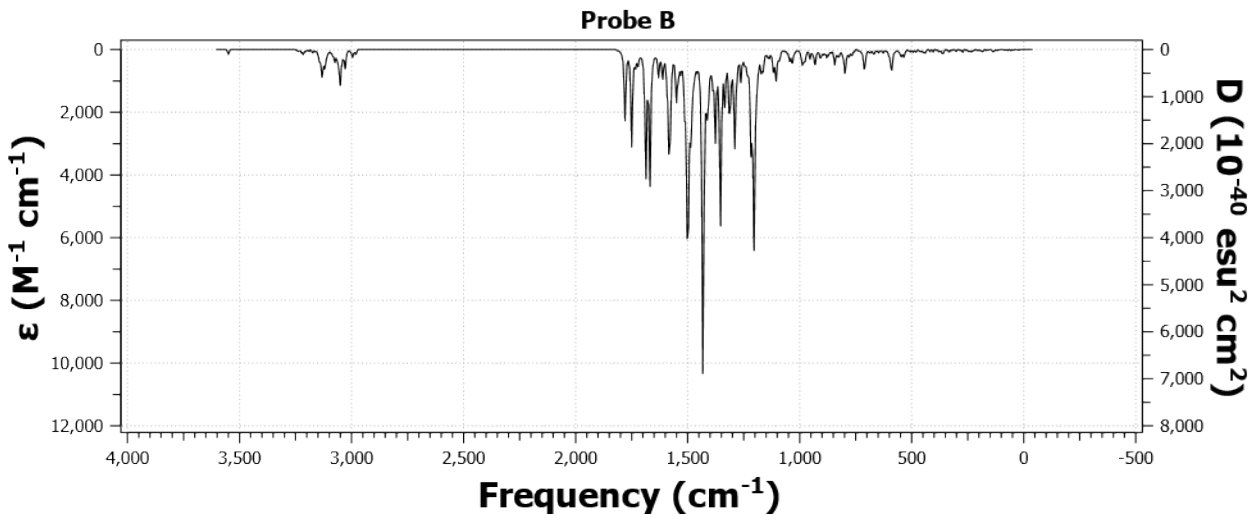


Figure S35. Calculated vibrational spectrum for probe BH^+ .

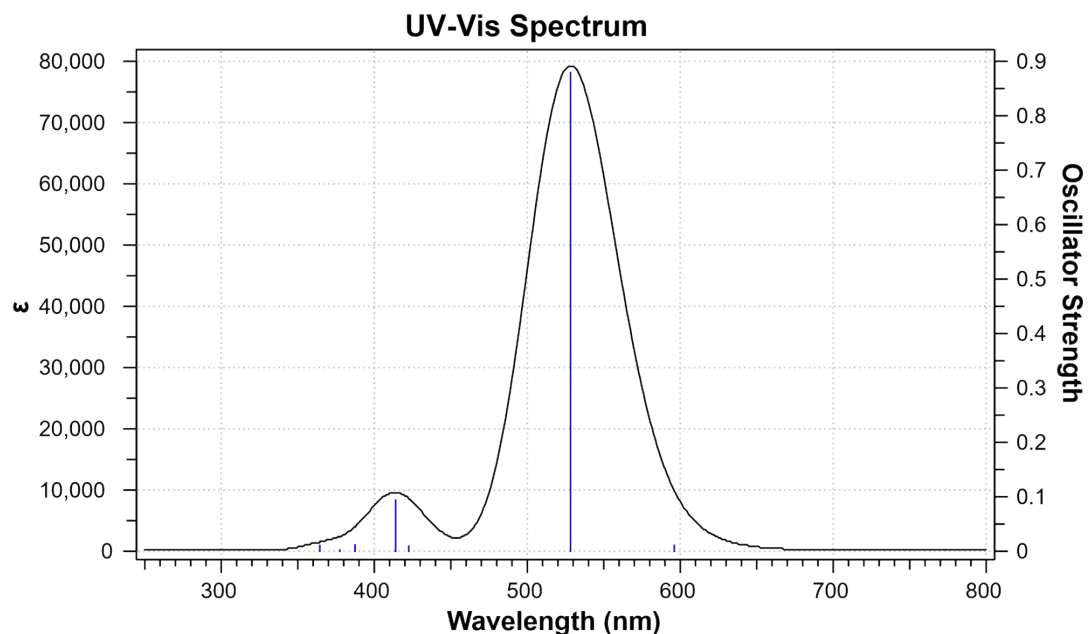


Figure S36. Calculated UV-Vis spectrum for probe BH^+ .

Table S8. Excitation energies and oscillator strengths listing for probe BH^+ .

Excited State	Nature	E(eV)	$\lambda(\text{nm})$	f	Orbital Transitions	Normalized Coefficient
1	A	2.08	596.07	0.0108	189->190	0.70462
2	A	2.347	528.26	0.8791	188->190	0.70029

Excited State	Nature	E(eV)	λ (nm)	f	Orbital Transitions	Normalized Coefficient
3	A	2.9347	422.47	0.0095	189->191	0.70349
4	A	2.9954	413.92	0.0939	187->190	0.68523
5	A	3.1999	387.46	0.0115	186->190	0.70194
6	A	3.2846	377.47	0.0022	187->191 188->191	-0.12575 0.69265
7	A	3.4027	364.37	0.0103	188->192 189->192	-0.2655 0.64383

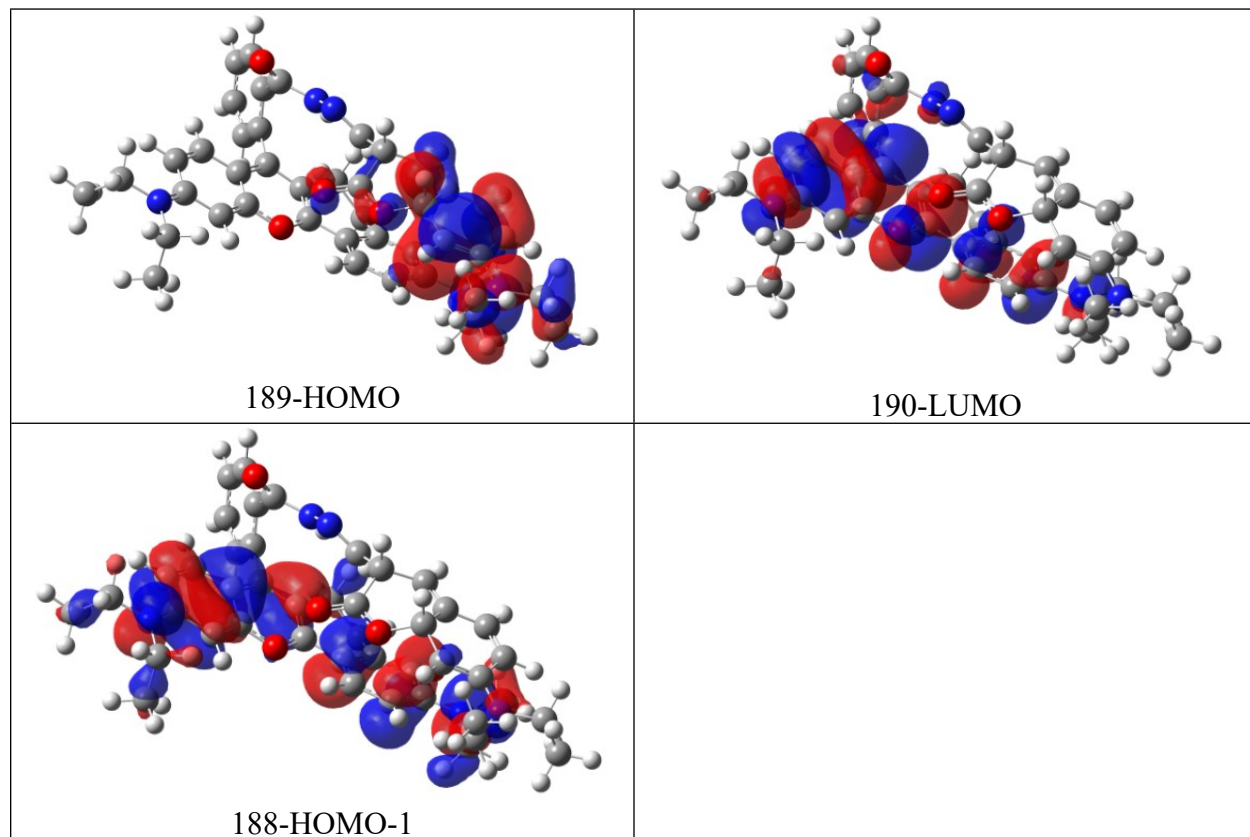
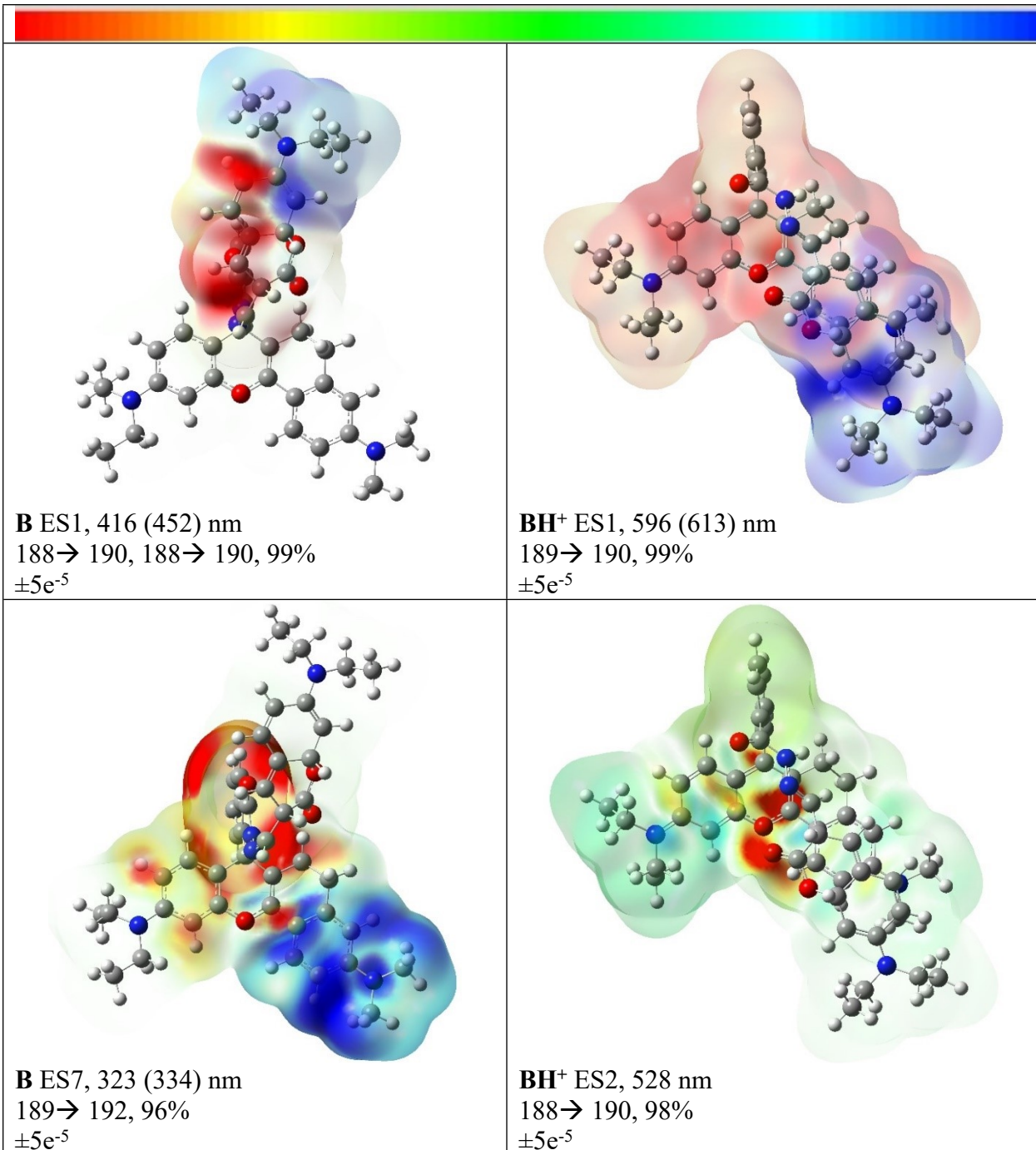


Figure S37. LCAOs for probe BH^+ involved with the transition noted as Excited State 1 in Table S12.



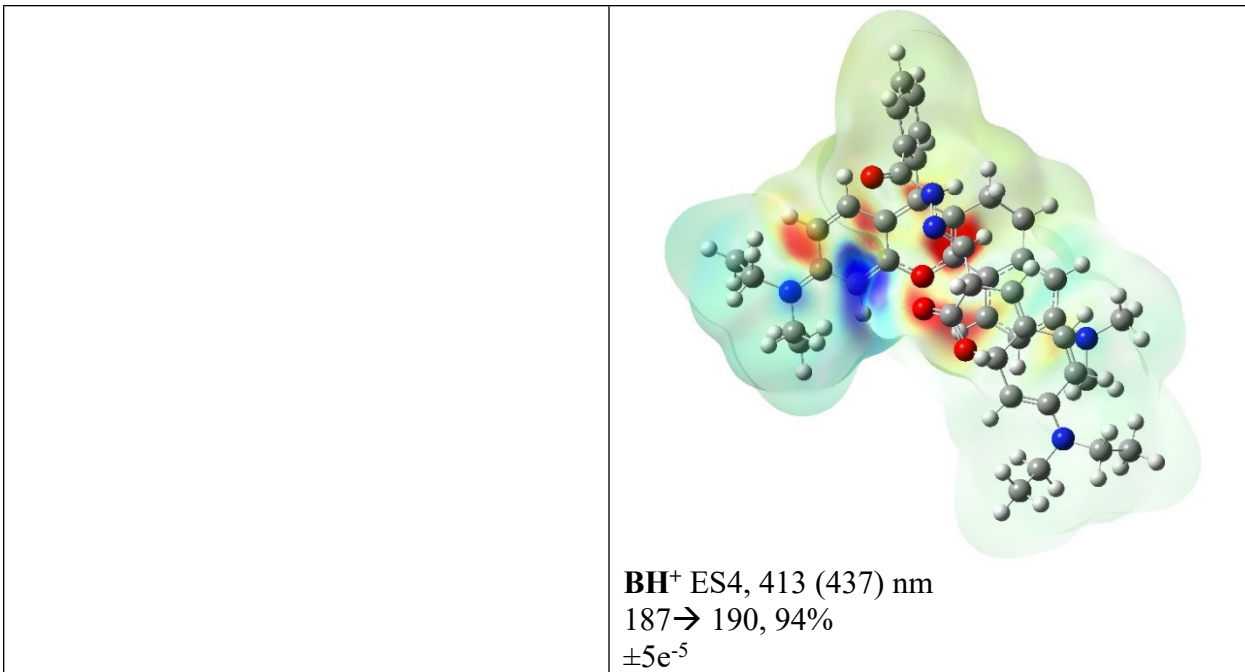


Figure S38. Current density difference drawings as isosurfaces of probes **B** (left) and **BH⁺** (right). The number of excited states (ES), the calculated (and experimental) wavelengths, and the transitions together with percentage contributions are listed. The range values for the color scale illustrated at the top of the figure are also listed.

14. Colocalization study in HeLa cells using Lysosome Tracker

The intracellular fluorescence shows the Pearson correlation coefficient (PCC) of 0.59 by the colocalization of probe A with lysosome tracker, Fig. S39. Thus, the intracellular fluorescence of probe A is predominantly localized in the mitochondria, and less so in lysosomes, as demonstrated by the strong co-localization of probe A red emission with IR-780's magenta emission, Fig. 3. In contrast, a PCC value of 0.44 is obtained between a comparison of the images in Channel 1 and III.

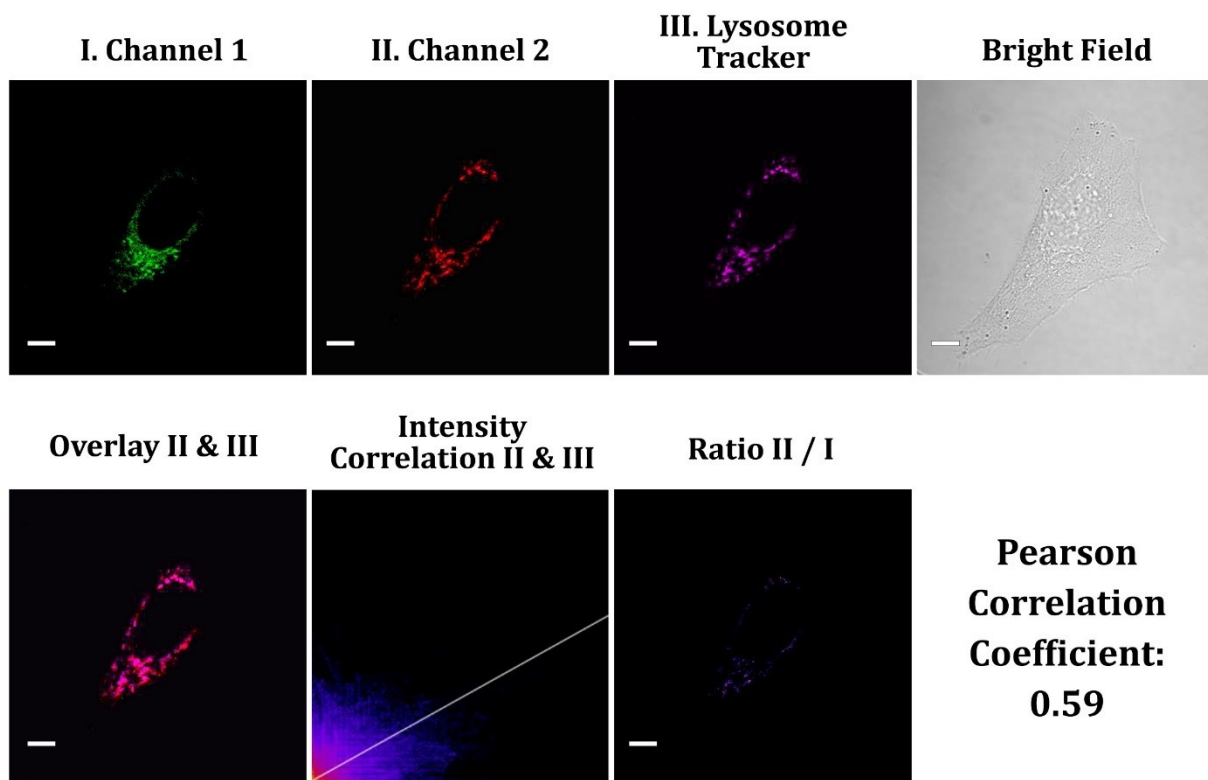


Figure S39. Fluorescence images of HeLa cells incubated for 2 hours with 10 μM probe A. The green channel (I) was used to observe the visible fluorescence of probes A in the 425-525 nm range, while the red channel (II) captured the near-infrared fluorescence from probe A (600-700 nm). Green channels utilized Alexa Fluor 405 nm and red channels utilized Alexa Fluor 559 nm excitation. The magenta channel (III) is used to detect near-infrared fluorescence from the lysosome-specific dye in the 700-800 nm range with Alexa Fluor 635 nm excitation. Scale bars represent 20 μm .

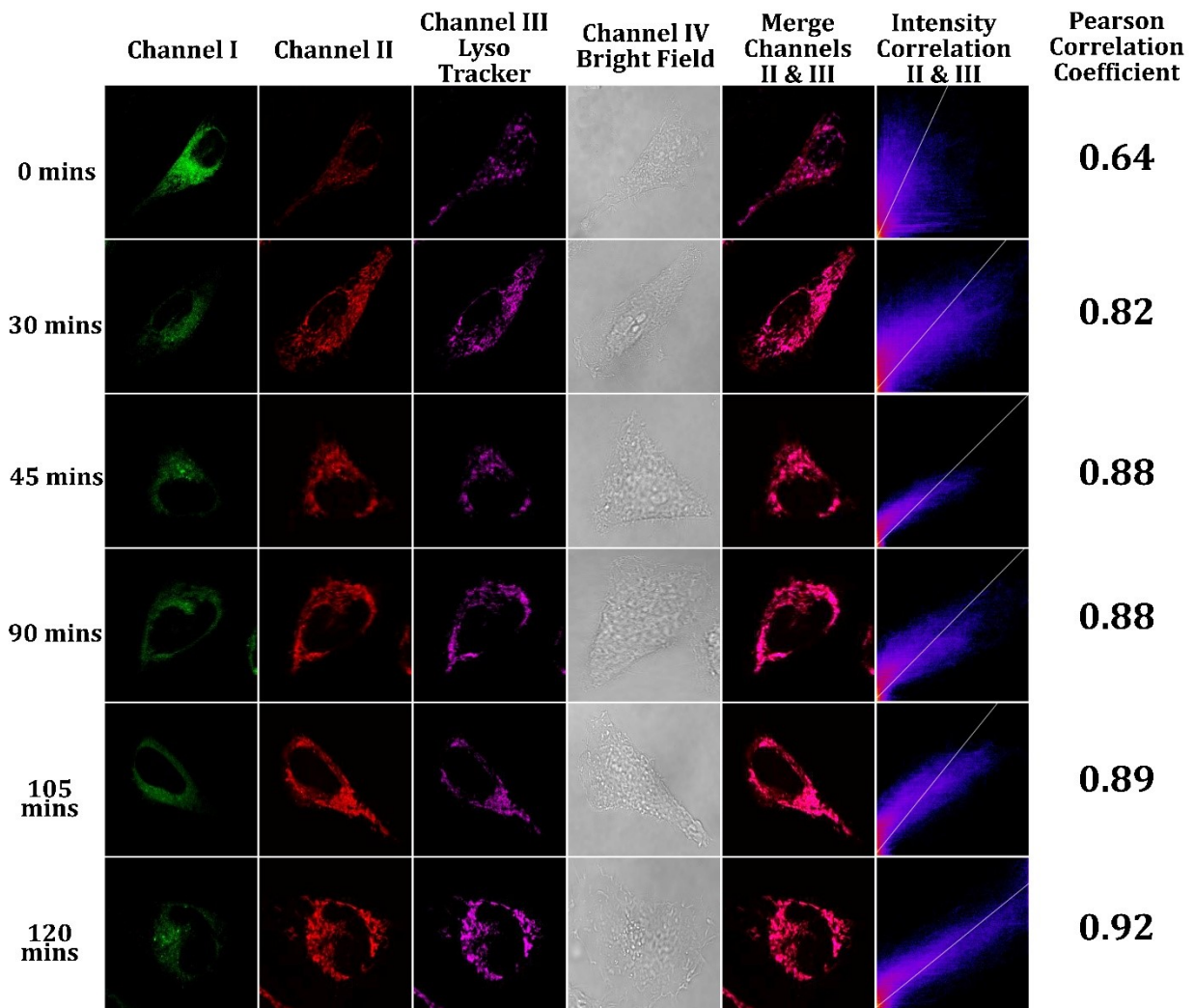


Figure S40. HeLa cells were first incubated with probe A and Lysotracker in DMEM for 30 minutes, followed by imaging using a confocal fluorescence microscope. Subsequently, the cells were treated with 5 μ M rapamycin for 30, 45, 90, 105, and 120 minutes, and fluorescence images were acquired at each time period.

Sample Name: Olivine pH 11.2 1

SOP Name: mansettings.nano

File Name: Example Results.dts

Dispersant Name: DMSO

Record Number: 445

Dispersant RI: 1.479

Date and Time: Thursday, May 8, 2025 3:21:59 PM

Viscosity (cP): 1.9910

Dispersant Dielectric Constant: 46.8

Temperature (°C): 24.9

Zeta Runs: 100

Count Rate (kcps): 119.1

Measurement Position (mm): 2.00

Cell Description: Clear disposable zeta cell

Attenuator: 10

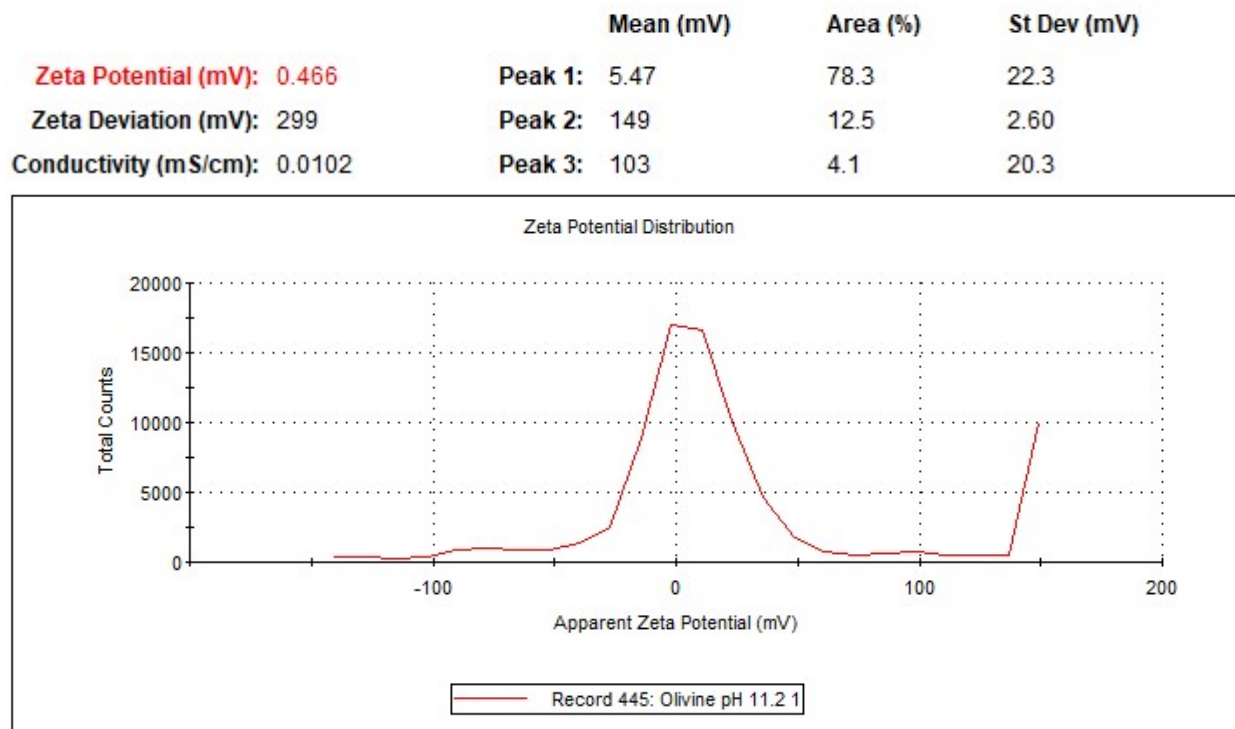
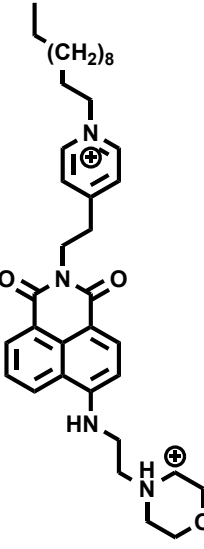
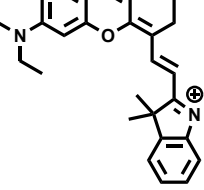
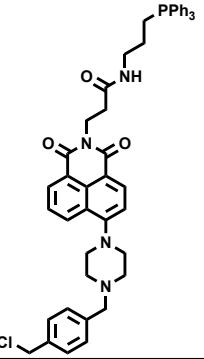
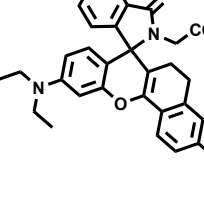


Figure S41. Measurement of the zeta potential of probe A in DMSO.

Table S9. Comparison of the proposed probe with other reported mitochondria targeting pH probes.

#	Molecular Structure	λ emission (nm)	pKa	Response Model	Application	Literature Review
1.		503-533	5.77	Single Channel	pH measurement in HeLa cells	Guo, L.; Liu, H.; Zhang, Z.; Shu, J.; Yu, X. Development of reaction-free and mitochondrion-immobilized fluorescent probe for monitoring pH change. <i>Sens. Actuators B Chem.</i> 2021 , <i>341</i> , 129962. https://doi.org/10.1016/j.snb.2021.129962
2.		727	7.6	Single channel	pH measurement HeLa cells	Mazi, W.; Yan, Y.; Zhang, Y.; Xia, S.; Wan, S.; Tajiri, M.; L. Luck, R.; Liu, H. A Near-Infrared Fluorescent Probe Based on a Hemicyanine Dye with an Oxazolidine Switch for Mitochondrial pH Detection. <i>J. Mater. Chem. B</i> 2021 , <i>9</i> (3), 857–863. https://doi.org/10.1039/D0TB02181D .
3.		525	6.18	Single channel	pH measurement in HeLa cells	Lee, M. H.; Park, N.; Yi, C.; Han, J. H.; Hong, J. H.; Kim, K. P.; Kang, D. H.; Sessler, J. L.; Kang, C.; Kim, J. S. Mitochondria-Immobilized pH-Sensitive Off-On Fluorescent Probe. <i>J. Am. Chem. Soc.</i> 2014 , <i>136</i> (40), 14136–14142. https://doi.org/10.1021/ja506301n .
4.		650	6.54	Single channel	pH variation in HeLa cells and Tumor in mice	Wang, T.-R.; Chen, Q.; Tang, M.-Y.; Zhang, Y.; Shen, S.-L.; Cao, X.-Q. Visual Monitoring of the Mitochondrial pH Changes during Mitophagy with a NIR Fluorescent Probe and Its Application in Tumor Imaging. <i>Spectrochim. Acta. A. Mol. Biomol. Spectrosc.</i> 2022 , <i>280</i> , 121496. https://doi.org/10.1016/j.saa.2022.121496 .

5.		748	7.27	Single channel	pH measurement in HeLa cells Ji, X.; Jin, Q.; Shi, Y.; Yang, X.-F. A Mitochondria-Targeted near-Infrared Fluorescent Probe for pH Monitoring in Living Cells Based on the Rhodamine-Hemicyanine Hybrid Structure. <i>Dyes Pigments</i> 2025 , 232, 112465. https://doi.org/10.1016/j.dyepig.2024.112465 .
6.		574	6.96	Single channel	pH measurement in HeLa cells and Zebra fish Qiu, J.; Zhong, C.; Liu, M.; Xiong, X.; Gao, Y.; Zhu, H. A Tunable pH Probe Scaffold Based on Sulfonamide Rhodamine and Its Application in Mitochondrial pH Research. <i>Sens. Actuators B Chem.</i> 2022 , 371, 132606. https://doi.org/10.1016/j.snb.2022.132606 .
7.		660, 465	4.43	Ratiometric response	pH measurement and viscosity monitoring in HeLa cells, fruit fly This work

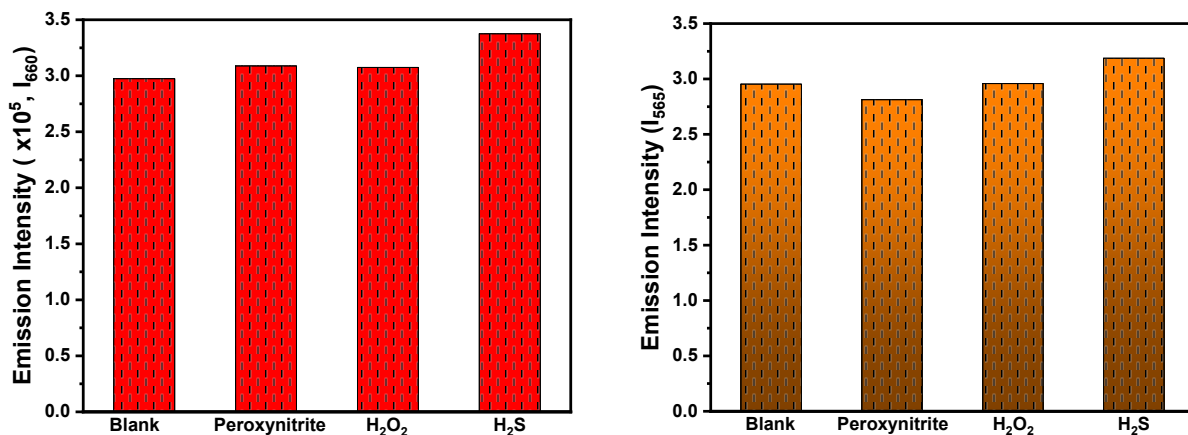


Figure S42: Fluorescence intensity of Probe A (left) and Probe B (right) in the absence and presence of 100 μM of peroxynitrite, H_2O_2 , and 100 μL of H_2S gas in PBS solution. Measurements were taken at pH levels of 7.2 using PBS buffer under excitation at 380 nm, and 400 nm, respectively. The rhodamine emission peak at 660 nm is used to indicate the emission intensity of probe A and the emission peak at 570 nm is used for the emission intensity of probe B.

For these analyses, the effect of reactive nitrogen species (RNS), reactive oxygen species (ROO), and reactive sulfur species (ROS) were tested using 100 μM of peroxynitrite, 100 μM of H_2O_2 , and 100 μL of H_2S gas in PBS, respectively. Peroxynitrite was synthesized using reported procedures.^{6, 7} Briefly, 3 mL of 0.6M sodium nitrite (NaNO_3) solution is mixed with 3 mL of 1.5 M sodium hydroxide (NaOH) solution and cooled in ice bath for 30 mins. In another glass vial, 1.5 mL of 0.5 M of hydrochloric acid is mixed with 1.5 mL of 2% w/v H_2O_2 solution. The second mixture is poured quickly into the first mixture and allowed to be stirred for 5 mins. The solution turned bright yellow in color. The pH is maintained at 9.0. The concentration of prepared ONOO^- was determined by measuring absorption at 302 nm using UV-visible spectrophotometer, (molar extinction coefficient value = $1.7 \times 10^3 \text{ M}^{-1}\text{cm}^{-1}$).² UV-Vis spectra of synthesized peroxynitrite at pH of 9.01 is presented in Figure below. The peak at 302 nm belongs to the peroxynitrite, and 350 nm belongs to the decomposition products.

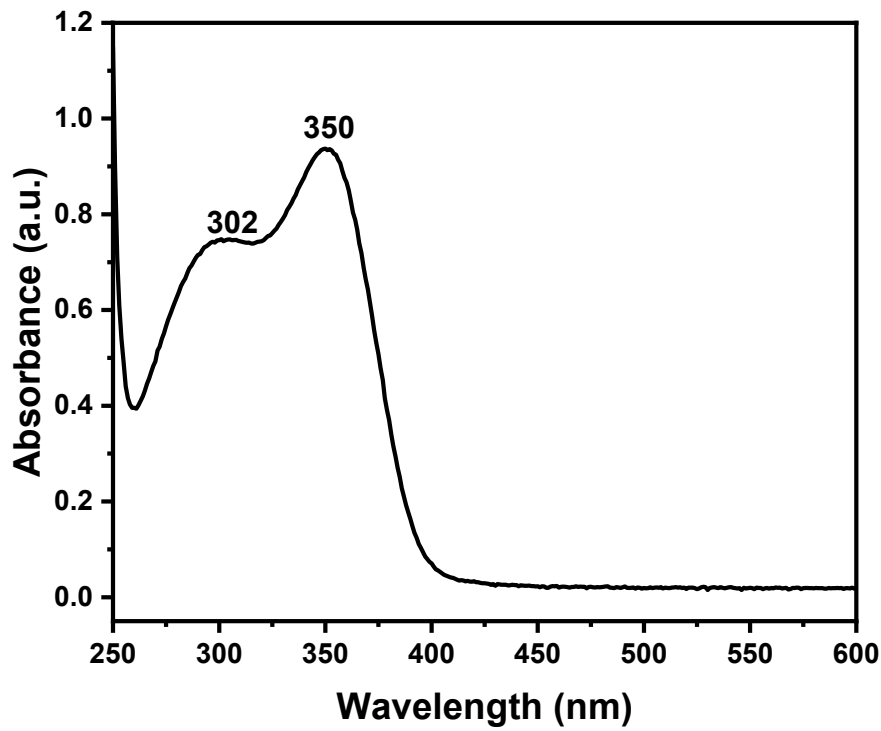


Figure S43. UV-visible spectra of synthesized peroxy nitrite.

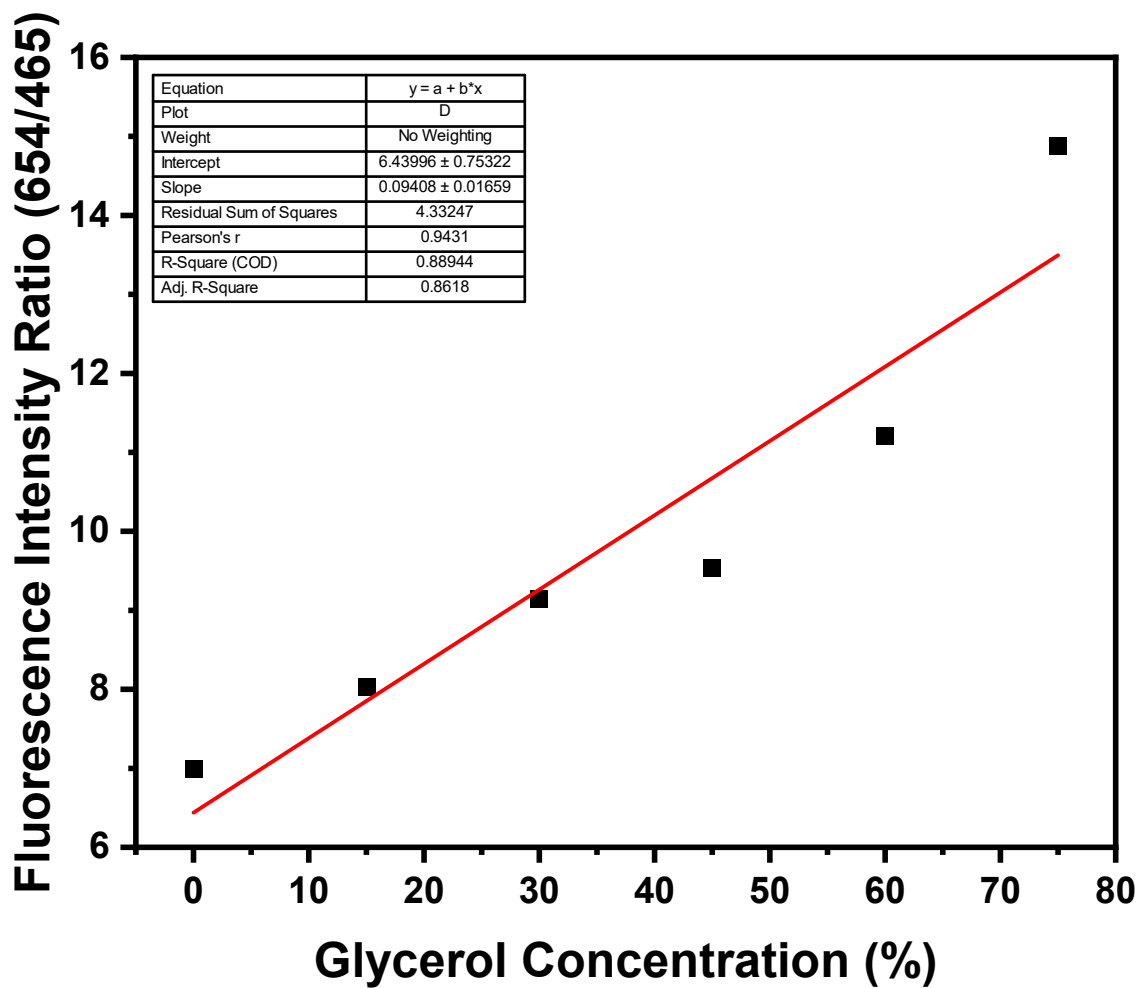


Figure S44. Fluorescence spectra of probe AH^+ in buffer (pH 3.50) with varying glycerol concentrations.

15. References

- (1) Brown, A. T.; Hallas, G.; Lawson, R. Synthesis of 6-(dimethylamino)tetral-1-one and 5-dimethylaminoindan-1-one. *Chem. Ind. (London)* **1981**, (7), 248.
- (2) *Gaussian 16, Revision A.03*; Gaussian, Inc.: Wallingford CT, 2016. (accessed).
- (3) Jacquemin, D.; Wathélet, V.; Perpète, E. A.; Adamo, C. Extensive TD-DFT Benchmark: Singlet-Excited States of Organic Molecules. *J. Chem. Theory Comput.* **2009**, 5 (9), 2420-2435. DOI: 10.1021/ct900298e.
- (4) *GaussView, Version 6.0.16*; GaussView, Version 6.0.16. Semichem Inc.: Shawnee Mission, KS., GaussView, Version 6.0.16. Semichem Inc. 2016. http://gaussian.com/g_prod/gv5.htm (accessed).
- (5) Macrae, C. F.; Bruno, I. J.; Chisholm, J. A.; Edgington, P. R.; McCabe, P.; Pidcock, E.; Rodriguez-Monge, L.; Taylor, R.; van de Streek, J.; Wood, P. A. Mercury CSD 2.0 - New Features for the Visualization and Investigation of Crystal Structures. *J. Appl. Crystallogr.* **2008**, 41, 466-470.
- (6) Robinson, K. M.; Beckman, J. S. Synthesis of Peroxynitrite from Nitrite and Hydrogen Peroxide. In *Methods in Enzymology*, Vol. 396; Academic Press, 2005; pp 207-214.
- (7) Saha, A.; Goldstein, S.; Cabelli, D.; Czapski, G. Determination of Optimal Conditions for Synthesis of Peroxynitrite by Mixing Acidified Hydrogen Peroxide with Nitrite. *Free Radical Biol. Med.* **1998**, 24 (4), 653-659. DOI: [https://doi.org/10.1016/S0891-5849\(97\)00365-1](https://doi.org/10.1016/S0891-5849(97)00365-1).